

NOLTR 64-53

*NOLTR  
64-53  
70N*

INITIATION OF REACTION IN EXPLOSIVES  
BY SHOCKS

Do not forward this copy to other activities  
without authorization of BuWeps (DLI-32)

**RETURN TO  
BUR. OF NAVAL WEAPONS  
TECHNICAL LIBRARY**

Dept. of the Navy  
Washington 25, D. C.

*AD. 474166*

**NOL**

4 OCTOBER 1965

UNITED STATES NAVAL ORDNANCE LABORATORY, WHITE OAK, MARYLAND

NOLTR 64-53

## NOTICE

Requests for additional copies by Agencies of the Department of Defense, their contractors, and other Government agencies should be directed to:

Defense Documentation Center (DDC)  
Cameron Station  
Alexandria, Virginia

Department of Defense contractors who have established DDC services or have their 'need-to-know' certified by the cognizant military agency of their project or contract should also request copies from DDC.

All other persons and organizations should apply to:

U.S. Department of Commerce  
Clearinghouse for Federal Scientific and Technical Information  
Sills Building  
5285 Port Royal Road  
Springfield, Virginia 22151

INITIATION OF REACTION IN EXPLOSIVES BY SHOCKS

By T. P. Liddiard, Jr. and S. J. Jacobs

**ABSTRACT:** Several solid high explosives are subjected to shocks of moderate amplitude, 10-50 kb. In general, these shocks are strong enough to cause chemical reaction, but not full detonation. The shock-producing system used is essentially that of the NOL standardized gap test. The acceptors (50.8 mm diam x 12.7 mm thick) are much shorter and are unconfined. Examples (photographic sequences) are shown of the acceptor response of several explosives at various entering shock pressures (stresses). The stress in the acceptor which just produces detectable reaction is determined from a plot of the break-out time of gaseous products of reaction from the acceptor as a function of the entering stress. The stress at which detonation is just produced in the acceptors is also determined. Threshold values for burning and for detonation also are obtained from graphs of the velocity of the acceptor undergoing chemical reaction as a function of the entering stress. Near the threshold for burning the velocity of the acceptor surface is very sensitive to the amount of reaction. This results in an abrupt change of slope in the velocity-stress curve at the critical stress for burning. The thresholds for burning and for detonation are compared with the 50% firing stresses obtained with the standardized gap test.

PUBLISHED DECEMBER 1965

EXPLOSION DYNAMICS DIVISION  
EXPLOSIONS RESEARCH DEPARTMENT  
U. S. NAVAL ORDNANCE LABORATORY  
WHITE OAK, MARYLAND

UNCLASSIFIED

NOLTR 64-53

4 October 1965

INITIATION OF REACTIONS IN EXPLOSIVES BY SHOCKS

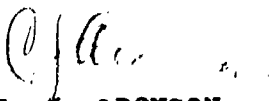
The experimental work described in this report was started under Project LACE at NOL for FY 1963 (Task NOL 260) and supported by the U. S. Atomic Energy Commission through a contract with the E. O. Lawrence Radiation Laboratory, Livermore, California. With the termination of Project LACE at NOL in 1963, the work was supported under BuWeps Task RMMO 51 042/212-1/F009-08-02 (Guided Missile Warhead Explosive Applications).

An immediate aim of this work is to determine the sensitivity of high explosives to burning and detonation under low-amplitude shocks. This could indicate under what conditions a warhead would become dangerous or fail to detonate with optimum effect. Although there are many possible stimuli that could cause burning or detonation, mechanical shocks are perhaps the most frequently encountered. Low velocity, weak impacts of missiles, such as accidental drops on ship decks or concrete runways, may cause unexpected warhead burning or firing. Low-amplitude shocks may adversely affect the reliability and efficiency of contact and penetrating types of warheads. The conditions which cause burning are as important as the conditions which cause detonation.

The identification of commercial materials implies no criticism or endorsement by the U. S. Naval Ordnance Laboratory.

The authors acknowledge with gratitude the fine work done by Mr. James Schneider in carrying out these experiments and by Mr. James Cliphant in assisting him. The careful preparation of the charges by members of the Chemical Engineering Division and the runs of the NOL standard gap test made by members of the Physical Chemistry Division are also gratefully acknowledged. The plastic bonded explosives were obtained through the courtesy of G. Dorough of UCLRL, Livermore, California.

J. A. DARE  
Captain, USN  
Commander

  
C. J. ARONSON  
By direction

NOLTR 64-53  
UNCLASSIFIED

TABLE OF CONTENTS

	Page
1. INTRODUCTION	1
2. EXPERIMENTAL PROCEDURE	
2.1 Test Arrangement	3
2.2 Observation	3
2.3 Explosive (Acceptor) Samples	5
3. RESULTS AND ANALYSIS	
3.1 Acceptor Response, Photographic Observations	6
3.2 Treatment of Data	10
3.3 Results	13
4. DISCUSSION OF RESULTS	
4.1 Shock Pressure for Initiation of Detonation	13
4.2 Shock Pressure for Initiation of Perceptible Reaction	14
4.3 Comparisons	14
5. GENERAL DISCUSSION	16
6. REFERENCES	18

TABLES		
Number	Title	Page
I	ACCEPTOR VELOCITY ( $U_a$ ) AND BREAK-OUT TIME ( $\tau$ ) FOR SEVERAL EXPLOSIVES AT VARIOUS ENTERING STRESSES ( $P_e$ ) WHICH CORRESPOND TO THE GAP LENGTH ( $S$ ) AND GAP STRESS ( $P_g$ ). $U_a^*$ IS THE CALCULATED ACCEPTOR VELOCITY WITHOUT CHEMICAL REACTION	19
II	THE THRESHOLDS OF BURNING ( $P_b$ ) AND DETONATION ( $P_d$ ) AND THE 50% FIRING PRESSURES ( $P$ ) OF THE STANDARD GAP TEST USING CONFINED ACCEPTORS	21

FIGURES		
Number	Title	Page
1	THE MODIFIED GAP-TEST ARRANGEMENT	22
2	DETONATION PRODUCED IN CAST COMP B-3 (UPPER ROW) AT $P_e = 47.0$ kb AND IN PRESSED COMP B-3 (LOWER ROW) AT $P_e = 35.0$ kb	23
3	FULL DETONATION PRODUCED IN LX-04-0 AT $P_e = 51.4$ kb	24
4	AN ALMOST COMPLETELY DETONATED TNT (PRESSED) ACCEPTOR AT $P_e = 57.0$ kb	25
5	PARTIAL DETONATION IN LX-04-0 AT $P_e = 41.2$ kb	26
6	MODERATE BURNING PRODUCED IN CAST COMP B-3 AT $P_e = 20.7$ kb	27
7	VIGOROUS BURNING IN PBX 9404 PRODUCED AT $P_e = 24.7$ kb	28
8	VIOLENT BURNING PRODUCED IN LX-04-0 AT $P_e = 38.6$ kb	29
9	VIGOROUS BURNING IN TETRYL AT $P_e = 17.4$ kb	30
10	A "PARTIAL DETONATION" IN PRESSED PENTOLITE AT $P_e = 14.1$ kb	31
11	PROFILES OF VIGOROUSLY REACTING ACCEPTORS: (A) PBX 9404 AT $P_e = 24.7$ kb, (B) TETRYL AT $P_e = 17.4$ kb, AND (C) PRESSED COMP B-3 AT $P_e = 24.0$ kb	32

CONTENTS (Con't)

Number	FIGURES Title	Page
12	PROFILES OF REACTING LX-04-0 ACCEPTORS: (A) VIOLENT REACTION AT $P_e = 38.6$ kb, (B) "PARTIAL DETONATION" AT $P_e = 41.2$ kb, (C) FULL DETONATION AT $P_e = 51.4$ kb	33
13	PROFILES OF "PARTIALLY DETONATING" ACCEPTORS: (A) PRESSED PENTOLITE AT $P_e = 14.1$ kb, (B) PRESSED COMP B-3 AT $P_e = 25.7$ kb, AND (C) PRESSED TNT AT $P_e = 51.8$ kb	34
14	METHOD OF DETERMINING THE STRESS IN THE ACCEPTOR FROM WHICH THE FREE-SURFACE VELOCITY OF AN UNREACTING ACCEPTOR ( $U_a^*$ ) CAN BE CALCULATED	35
15	INSTANTANEOUS VELOCITY ( $U_i$ ) OF THE ACCEPTOR AS A FUNCTION OF DISPLACEMENT (X) FOR COMP B-3 CAST	36
16	INSTANTANEOUS VELOCITY ( $U_i$ ) AS A FUNCTION OF DISPLACEMENT (X) FOR PRESSED COMP B-3	37
17	BREAK-OUT TIME ( $\tau$ ) AND ACCEPTOR VELOCITY ( $U_a$ ) AS FUNCTIONS OF THE ENTERING SHOCK STRESS ( $P_e$ ) <sup>a</sup> FOR TETRYL	38
18	$U_a$ AS A FUNCTION OF $P_e$ FOR PRESSED AND CAST TNT	39
19	$\tau$ AND $U_a$ AS FUNCTIONS OF $P_e$ FOR PRESSED AND CAST PENTOLITE	40
20	$\tau$ AND $U_a$ AS FUNCTIONS OF $P_e$ FOR PRESSED AND CAST COMP B-3	41
21	$\tau$ AND $U_a$ AS FUNCTIONS OF $P_e$ FOR CAST AND PRESSED 60/40 CYCLOTOL	42
22	$\tau$ AND $U_a$ AS FUNCTIONS OF $P_e$ FOR PBX 9404	43
23	$\tau$ AND $U_a$ AS FUNCTIONS OF $P_e$ FOR LX-04-0 AND LX-04-1 <sup>a</sup>	44

## 1. INTRODUCTION

This paper is concerned with an experimental study of the initiation of reaction in explosives by shocks of moderate amplitude. High-speed photography with auxiliary lighting is used. The study covers the borderline region of shock pressures between an upper limit where transition to detonation occurs, and a lower limit where no apparent reaction is detected. The study was undertaken because there has been a need for a closer look at what happens when the initial shock stimulus is insufficient to cause detonation, but sufficient to cause burning or even violent explosion. The method is a simple extension of photographic studies on gap-type experiments<sup>1</sup>.\*

Results of critical gap (50% point) tests have shown that typical shock pressures of 10 kilobars or so will build up to detonation in a sensitive explosive like pressed 50/50 pentolite. However, a pressure of 40 kb or more is required for build up in an insensitive explosive like cast TNT<sup>2</sup>. These pressures lead one to question whether the usual gap-test results fall in the right range of pressures to adequately describe the accidental initiation of reaction in ordnance items. In most, if not all, cases where warheads or warhead models have been subjected to impact loading, fires or non-detonating explosions are found to occur when impact shocks are more nearly 1 to 5 kb<sup>3</sup>. The wide difference between shocks necessary to cause detonation and those which start fires suggested that it would be worthwhile to carry out small-scale studies on explosives subjected to mild shocks. Shocks of this lower amplitude can be conveniently produced by the usual donor explosive and barrier of the familiar gap-test experiment. Inasmuch as a donor-barrier system had already been calibrated for peak shock pressure in a plastic barrier as a function of length, this system was employed for convenience<sup>4</sup>. The shocks generated in an explosive by this cylindrically symmetric system are neither plane nor of uniform amplitude, either radially or axially. However, it had been established that the measured peak pressure causing detonation in this system is very near to what is obtained in more precise plane-wave systems<sup>1</sup>. This may be taken to mean that the details of shock-to-detonation transition are dependent mostly on pressure and its duration, and are not affected particularly by geometrical details of the system. Thus, the simpler geometry was attractive for use in these preliminary studies.

Aside from practical tests, past work on initiation of reaction, short of detonation by mechanical shock, has been somewhat limited. The impact machine, an example of a practical test, certainly measures the ignitability of explosives under

---

\* References may be found on page 18.

compression loading. This device has not yet been controlled sufficiently, however, to use it as a basis for detailed study. Also, it does not lend itself to camera synchronization. The most successful approaches, to date, have been the various moderate-velocity impact experiments performed at UCLRL<sup>3</sup>. In fact, it is the reported work of the LRL group which suggested to us that the present study might be of value. Eichelberger and Sultanoff<sup>4</sup> published a single Kerr cell photograph showing smoky gas blow-off from a short cylinder of explosive which had not yet detonated. The experimental set-up is quite similar to that used here and the result is much the same as we obtained when build-up of reaction is on the verge of detonation. But these authors did not pursue their work in the direction of weaker shocks. They were more concerned with the study of the initiation phase when shocks are of sufficient amplitude to cause detonation in long columns. Similarly, Clay<sup>5</sup> has published measurements of pressure from short cylinders to show the pressure produced in the pre-detonation phase of build-up. He, however, gives little or no data on the result of weakly shocking an explosive. Napadensky<sup>6</sup> has carried out photographic studies in the weak-shock range in which the acceptor was crushed between a steel driver plate and a steel platform. Unfortunately, the detailed results of this work are unreported in the accessible literature.

In the present experiments a short cylinder of explosive is shocked by a wave transmitted by a donor charge through a calibrated barrier of PMMA\*. The motion of the free surface of the acceptor is observed by a framing camera. In the absence of reaction within the acceptor the free surface is found to move with an axial velocity which agrees with that calculated for the material under shock loading; i.e., twice the particle velocity in the transmitted shock. When reaction is present, due to shocks of higher incident pressure, the axial surface velocity is greater than the calculated (unreactive) velocity. In addition, a dark cloud of smoke is usually seen to emerge from the sample. At still higher shock inputs transition to detonation is observed. The axial velocity of the gas and other material blowing off then approaches, as a limit, the typical escape velocity for gas from a detonating charge. A number of explosives have been studied in both cast and pressed charges. Some photographic examples of the results are presented. Results obtained from free-surface velocity measurements (or break-out time of gases), as a function of entering shock pressure, are presented in a series of graphs and tables.

\*Polymethyl methacrylate (Plexiglas, Lucite, or Perspex).

## 2. EXPERIMENTAL PROCEDURE

### 2.1 Test Arrangement

The modified gap test used throughout this investigation was based on the donor-gap system of the NOL Standard Gap Test<sup>8</sup>. For that test the peak pressure in the gap of PMMA, along the axis, has been calibrated as a function of gap length. (Recent checks have shown substantial deviations from the calibration in Ref. 2. A later calibration is used here.) The modified gap test and arrangement for photographing each experiment is shown in Fig. 1. Two charge set-ups were tested simultaneously to conserve light sources. An appropriately placed mirror, as sketched, supplied an end-on view of the acceptors.

The 51-mm diameter, 51-mm long, donor charges were of tetryl, containing 1% graphite, and pressed to a density of  $1.51 \pm 0.01$  g/cm<sup>3</sup>. The detonators were J-2 special blasting caps\* connected in series and fired by the sudden discharge of a 4  $\mu$ f capacitor charged to 6 kv. The gaps were machined to length from 51-mm diameter (cast) rods of PMMA stock\*\*. [Rods formed by extrusion were found to show prominent residual stress patterns under polarized light. Although not proven, this might affect the results at low shock amplitudes. Thus, extruded rods were avoided.] A baffle of 13-mm thick plywood was used to impede the forward flow of gases formed by the detonating donor. Even with the baffle it was difficult to keep these gases from prematurely obscuring the acceptor in the side view. The use of a higher density or thicker baffle was avoided, however, because either variant might appreciably alter the pressure calibration.

### 2.2 Observation

The observations were made with a high-speed, focal plane shutter, framing camera<sup>8,9</sup>. Front-lighting was used in all cases, the light source being an argon-filled, explosive flash lamp. The plywood body of the light source was in the shape of a truncated, square-based pyramid; 61-cm long, 10 cm x 10 cm at the back end, and 20 cm x 20 cm at the front (inside dimensions). The inside surfaces were lined with aluminized polyester film and 50-mm wide strips of 3-mm thick EL506C (plastic) explosive\*\*\*

\*Manufactured by Hercules Powder Co., Wilmington, Delaware.

\*\*There appears to be no significant difference in performance between gaps formed by stacks of 0.25-mm thick "cards" and solid rods of the essentially similar material, i.e., Lucite or Plexiglas.

\*\*\*Manufactured by E. I. duPont deNemours & Co., Wilmington, Del.

were placed down the middle of two opposing inside surfaces. The plastic explosive strips were folded at the rear of the source and brought in contact with a 51-mm diameter, 25-mm thick tetryl booster at the center of the back. Such a system gives high luminosity for more than 100  $\mu$ sec, using a relatively small amount of high explosive<sup>10</sup>. Back-lighting also was obtained, in most of the shots, by reflecting some of the light from a white or gray cardboard background. This gave some outline to the frames for reference purposes and aided in outlining the acceptor blow-off. In many cases, however, the changing nature of the surface of the acceptor made it difficult to obtain good contrast throughout an experiment. The camera permits up to 216 frames to be recorded, but only about one-half that number of frames was obtained for the required observation time of 100  $\mu$ sec at a frame rate of 920,000 fps.

Although the camera has been previously described<sup>8,9</sup>, some aspects of the principle of its operation are given here to help the reader understand the results shown in Figures 2-10 to be described later. First, the camera may be considered to be a hybrid, combining some aspects of a smear camera with those of a framing camera. Each frame is recorded by a narrow-slit, focal-plane shutter, which at  $9.2 \times 10^5$  fps, crosses the picture area from left to right in 6.53  $\mu$ sec. In most cases the shutter slit is 0.25 mm wide leading to an exposure time of each image element of 0.065  $\mu$ sec. The frame rate stated above is obtained by combining six shutters, each delayed by 1.09  $\mu$ sec relative to its predecessor. At 1.09  $\mu$ sec after the entry of shutter No. 1 on the first frame, shutter No. 2 enters the second frame; 1.09  $\mu$ sec after shutter No. 6 enters the sixth frame, shutter No. 1 enters frame 7 and so on throughout the picture taking cycle. The relatively long scan time of each shutter results in a fairly large amount of image motion, i.e., time distortion during the exposure of a frame. For moving waves, such as shocks or detonations, this time distortion is somewhat like the trace in a smear or streak camera. The fine details of motion within a frame frequently can be resolved and interpreted, thereby, just as one interprets the x-t data of a smear camera. In the set-up of Figure 1, the images of the individual acceptor charges (51-mm diam) are crossed by shutter slits in about 1.6  $\mu$ sec. This accounts for the tilted wave fronts seen in the records; for example, the sloping of the bottom of the air shock seen in Fig. 3. In the cylindrical geometry employed in these studies one would expect, and generally finds, the motions to be symmetrical about the acceptor axis. Thus, the time base resulting from the scanning slits is used to advantage to interpolate wave motions within a given frame. For additional discussions of data retrieval, the reader is directed to References 8 and 9.

### 2.3 Explosive (Acceptor) Samples

The explosive samples used, listed in Tables I and II, were held to close tolerances for density. This, for a particular explosive, was within  $\pm 0.003$  g/cm<sup>3</sup> in all cases, except where noted. Wherever possible, all acceptors in a particular explosive series were cut from the same pressing or casting. To insure uniformity in the pressed samples, an isostatic press was used, the end pieces being discarded in the cutting and machining process. Each acceptor was weighed on an analytical balance. The dimensions of each acceptor were measured to  $\pm 0.005$  mm.

The PBX and LX explosives (described in Table I footnotes) came in the form of large aggregates of explosive and binder. The other explosives were sieved before pressing or casting, passing through a U. S. Standard 70 mesh (210 $\mu$ ) sieve and being retained on a 100 mesh (149 $\mu$ ) screen. The tetryl (for acceptors not donors) was ungraphited and pressed to 95.3% of the theoretical maximum density, TMD. This was the highest density obtainable for this material with the existing press. Nearly 98% TMD was obtained with TNT, using the same pressure. Here, though, the explosive, the mold, and the water in the isostatic press were preheated to 60°C before pressing. Heating apparently softens the TNT sufficiently to give high densities. No appreciable increase in density is obtained by preheating in the case of tetryl; it is apparently too far below the melting point at 60° to soften. However, all the TNT containing explosives in the series responded to preheating and relatively high densities were obtained.

The Composition B-3 was commercially made, being delivered in the form of cast chips\*. This material was remelted and while solidifying was stirred in a Sigma Mixer to produce granules. The granulated bulk then was sieved to size, i.e., to the range of 149 to 210 $\mu$ . Both pressings and castings were prepared from this batch. However, it is possible that most of the particles of RDX, in the pressed material, still remained in a matrix of TNT after reprocessing. Because of this, additional tests were made on an essentially equivalent dry blend of cyclotol; 58.5% RDX, 41.5% TNT by weight (actual analysis). The only significant difference between this material and Composition B-3 is in the particle size of the RDX. The 50/50 pentolite, for both pressed and cast charges, was composed of granular PETN and TNT. The TNT was from the same sieved batch that was used in making the "pure" TNT and cyclotol acceptors. An analysis of the

---

\*Composition B-3 contains no wax and is composed of 59.5% RDX and 40.5% TNT  $\pm 1.0\%$  by weight. The median particle diameter of the RDX is 65 to 80  $\mu$ .

blended pentolite, before pressing or casting, gave 48.8% PETN and 51.2% TNT by weight. The TNT, sieved from NOL Lot No. X-412 and labeled CH 5294, had a set point of 80.2°C.

To prevent cracking on cooling, 0.25% nitrotoluene by weight was added to the pentolite, Composition B-3, and 60/40 cyclotol melts. It was not necessary to use nitrotoluene in casting TNT and it was left out in this case.

### 3. RESULTS AND ANALYSIS

#### 3.1 Acceptor Response, Photographic Observations

Estimates of the magnitude of the chemical reaction in the acceptor may be obtained from the photographic records: (a) by the amount of gas or black smoke\* evolved from the free surface when it moves off, (b) by the time of emergence of gas after the shock reaches the surface, (c) by the presence of luminous air shocks when transition to detonation has occurred, and (d) by measurement of the axial velocity of surface blow-off. Before presenting details on how quantitative measures of the effects of reaction have been obtained, it is best that we first describe, in a general way, the responses that have been observed. Depending on the extent of reaction, but also to some degree on the nature of the explosive, the character of the surface blow-off may take several different forms. When the entering shock produces little or no reaction, the surface develops a dome shape. Because of surface changes, this dome reflects more light and, therefore, appears generally lighter in tone than the unshocked explosive. With small amounts of reaction, black smoke, in many instances, breaks through the surface of this dome after motion begins; a definite proof of reaction. At a higher shock amplitude a black or grey dome can develop almost immediately. When the shock is high enough to produce detonation before the surface is reached, a luminous zone of shocked air is formed. This shock then continues to move axially above the escaping products. At a still greater amplitude of shock, the entire charge detonates and luminous air shocks move laterally as well as axially.

Examples of acceptor behavior are shown in the photographic sequences of Figs. 2-10. These records are discussed below to point out details which appear to be significant. Some of these are not immediately obvious without being pointed out.

---

\*All explosives reported here are deficient in oxygen; the detonation products contain free carbon and therefore show up as a black smoke.

NOLTR 64-53  
UNCLASSIFIED

Fig. 2 shows two sequences of the initiation to detonation in Composition B-3. The upper row shows the cast explosive with an initial shock amplitude of 47.0 kb. Frame A shows the 12.7-mm thick acceptor sitting on the Plexiglas barrier. In Frame B a luminous air shock, characteristic of detonation within the sample, is forming at the free surface. The sloped black line seen on the periphery of the charge is the lateral arrival of the internal shock at the acceptor surface. (These shocks are normally symmetrical about the axis. However, due to slit motion from left to right they appear with a slanted time trace.) The formation of air shock is followed by mushrooming of the sides of the charge. In Frame C a detonation reaches the lateral surface when the camera slit was about 0.7 times the distance across the charge. The air shock then spreads as the slit continues to move across the charge. In Frame D the corresponding slit lags that of the previous frame by about 1 usec and, therefore, the lateral air shock is seen to develop about 0.3 times the distance across the charge. The end shock has now fully spread over the charge. From the location of the breakout of detonation at the sides, it appears that transition to detonation at the axis was complete at about 10 mm from the barrier-acceptor interface.

In the lower sequence the charge of pressed explosive was more sensitive to shock initiation. With an initial pressure of 35.0 kb, transition to detonation occurred about 7 mm above the barrier, as inferred from the lateral breakout in Frame C. This frame shows very clearly the origin of a narrow dark band which is very often seen in the lateral shock from deflagration-detonation transition (DDT) records. We see in Frame C that the detonation, proceeding laterally from the axis where it is first formed, has crossed the boundary between shocked and unshocked explosive and that the demarcation line between the two zones is preserved in the air-shock front for many microseconds. Frame B, particularly the top view in the mirror, is an interesting "chance" photograph. It shows the air shock a small fraction of a microsecond after formation as a disk about 7 mm in diameter. This is surrounded by a dark ring and then a bright ring of detonation light. The latter light is seen through a layer of yet unexploded material. A close look at the surface in Frame C also shows detonation light scattered through the surface as a ring ahead of the air shock.

Fig. 3 shows a similar sequence for a plastic bonded explosive (X-04-0) with an entering shock of 51.4 kb. The late frames of this sequence show the dark product gas zone following the brightly shocked zone at the tip of blow-off.

Fig. 4 shows the first departure we have observed from the usual DDT picture. In this example pressed TNT, with an entering

shock of 57 kb, has detonated prior to Frame D as evidenced by the bright air shock. One also sees the laterally moving shock within the acceptor arriving at the explosive surface. This is indicated by the slanted trace in Frame D. In Frame E a second shock has arrived at the side. This originated from the high pressure zone accompanying detonation near the axis. This is seen as a trace with a downward slope. Here the shock was not strong enough to initiate detonation laterally. As seen before and in the ensuing frames, the explosive forming the sides of the cylinder merely moves away without evidence of reaction. This result has been seen before on longer acceptors, and has usually been reported as the absence of a backward detonation after transition. The absence of backward detonation has usually been attributed to charge diameter.

Fig. 5 shows, for LX-04-0, that the lateral detonation in that explosive is absent when the entering shock strength is reduced. In this case, the entering shock is 41.2 kb, about 10 kb lower than for Fig. 3. Even though transition has occurred in the forward direction, the detonation has not spread laterally. We now see a central core of black product gases surrounded by an envelope of lesser darkness, the latter appearing to consist of particles of unreacted explosive intermixed with smoky gas products. Near the base of the vertically rising column there is no evidence of product gases mixing with unreacted explosive until nearly the last frame is reached. The shock luminosity near the tip disappears in Frame G. This may be due to jetting of product gases into the shocked air or merely a slowing down of the air shock. The luminosity, seen in Frames I and J, occurs when the gas column reaches the overhead mirror. This is attributed to shock reflections off the mirror.

Fig. 6 is an example of surface blow-off near the lower limit for observable reaction. In this case the HE is cast Composition B-3, the entering shock strength 20.7 kb. The shock has reached the free surface in Frame C and the material set into motion is seen to be much whiter than before shocking. The dome of HE moves upward with no apparent evidence of reaction until in Frame H, 33  $\mu$ sec after motion begins, fissures are seen to open up and black smoke emerges. More fissures open later and more smoke emerges, but the smoke does not move with any great excess spread relative to the surface. (The cloud which enters from the lower right in Frame G to obscure most of the front view in the last frame is due to product of explosion of the original donor charge.) Even before the fissures permit gas to escape, it is possible to infer that gas had evolved as a result of reaction by comparing the upward velocity of the dome with the velocity which would have been found if no reaction had occurred. Without reaction the maximum

dome velocity (on axis) would, in this case, have been 0.48mm/usec. The actual velocity found (see Table I G for Shot 47T) is 1.22 mm/usec, over 2 times as great. The added speed is the result of the mild explosion within the cylinder. Lack of any evidence of reaction in the outer surface layers may be attributed to quenching of reaction by the rarefaction waves reflected at the surface when the shock reaches it.

Fig. 7, for PBX-9404 at 24.7 kb initial shock strength, shows unmistakable evidence of internal reaction in the measured dome velocity of 2.62 mm/usec when the zero reaction predicted value would be less than 1/3 as great. There is none of the very black smoke emergence despite this significantly augmented velocity. There is darkening of the upper part of the dome which suggests the presence of smoke permeating fragments of unexploded HE. An attractive hypothesis to explain this result is that reaction has occurred in localized regions throughout the central part of the charge. The expansion of gas within these pockets to swell up the explosive would explain the formation of the dome.

In Fig. 8 we return to LX-04-0 now with an entering shock of 38.6 kb, which is but 2.6 kb lower than that for Fig. 5. The result somewhat resembles that of Fig. 7 with fairly definite mixing of smoke and unburned particles. The tip of the dome appears to be unburned HE seen by reflected light rather than a luminous shock or flame. (Note that the tip is lightest on the side facing the argon candle.) It appears to be material spalled from the surface which detaches from the remainder of the moving surface at about Frame F. The maximum upward velocity, 4+ mm/usec is probably too low to produce luminous shocks, but this possibility is not completely ruled out.

In Fig. 9, pressed tetryl at an entering pressure of 17.4 kb, we again see black smoke. This time it is formed almost immediately after the shock reaches the surface. The maximum velocity along the axis is 2.5 mm/usec. This cannot account for the delayed luminous zone which develops at the tip in Frame F or G. Since the blow-off apparently is composed of gaseous products and finely divided carbon, the luminosity suggests that the reduced products of explosion are burning in shock-heated air. The shock temperature, estimated at about 3000°K, is certainly adequate for ignition. (Reflected light has been ruled out because the tip is fairly uniformly bright, even though the external light source is to the right.)

In the last example, Fig. 10, the explosive is cast pentolite; initial shock pressure, 14.1 kb. This result resembles Fig. 5. The axial velocity of the tip is about the same. There is the smoky appearing center surrounded by a

gray granular envelope. There is, however, an hour-glass appearance to the column escaping from the center of the charge, as in Fig. 9. Here, as in Fig. 4, a backward moving wave is seen, Frame D, indicating a second pressure pulse. This pulse moves radially from the detonation which produced the bright air shock seen in Frame C. However, no lateral detonation developed as in Fig. 4.

Representative outlines of the blow-off at 6.5  $\mu$ sec intervals have been superimposed in each of the sketches of Figs. 11-13 to compare, more compactly, the response of a number of explosives. In Fig. 11 three different explosives are compared at about the same mean axial velocity, 2.5-2.6 mm/ $\mu$ sec. Fig. 11a (taken from Fig. 7, PBX 9404) shows a more or less spherical blow-off indicating a fairly large radial component of motion. Figs. 11(b) and 11(c) show progressively less spreading with a fairly small radial component of motion for the pressed Comp B-3 of 11(c). Fig. 12 shows how contours change with change of shock pressure for LX-04-0 as a representative sample. In Fig 12(a), below the detonation limit, the top is quite rounded. When part of the sample has detonated, 12(b), the top is flattened and broadened. Complete detonation, as illustrated in 12(c), show a substantially greater radial motion of the blow-off from the end as well as the typical high lateral motion of detonation from the sides of the charge. Fig. 13 compares three explosives which had partially detonated. The profiles which result are quite different. No doubt there is an interesting problem hidden here in the relation of the profiles to the details of what has happened to the explosive. We make little attempt at explanation beyond what has already been said. One thing is clearly common to all the explosives studied. The measured axial velocity of surface blow-off increases monotonely with the entering shock strength. The axial blow-off velocity is, therefore, a convenient variable to characterize the extent of reaction induced by the shock.

### 3.2 Treatment of Data

For a description of the response of the acceptor to shock, a number of pressures and velocities will be used. They are defined as follows:

- $P_g$  peak pressure in the **PMMA** gap incident on the acceptor explosive.
- $P_e$  initial peak pressure transmitted to the explosive acceptor.
- $P_b$  peak pressure transmitted to the acceptor which causes perceptible burning or reaction.

- $P_s$  minimum peak pressure transmitted to the acceptor for which transition to detonation is evident.
- $U_i$  instantaneous axial velocity of the material blown off the free surface of the acceptor. This velocity is a function of time or distance traveled.
- $U_a$  axial velocity of the material blow-off after 50 mm of travel.
- $U_a^*$  axial velocity of the free surface which would be produced by  $P_e$  if no reaction occurred.
- $p_a^*$  pressure in shock arriving at acceptor free surface if no reaction occurred.
- $u$  particle velocity.

We also define a time,  $\tau$ , as the interval between shock arrival at the surface and escape of smoke.

The magnitude of  $P_g$  is obtained from the gap length by the calibration of the donor gap system as given in Ref. 7. This relation is reproduced in part in Fig. 14. The value of  $P_e$  is obtained from  $P_g$  by graphical solution of the shock boundary conditions using P-u Hugoniot relations for the unreacted explosive and the PMMA. The method is described in Ref. 1. The unreacted Hugoniots for TNT and Composition B-3 used here were taken from References 11 and 12. The Hugoniots for the other explosives are approximations based on the shock vs particle velocity data for TNT or Composition B-3. Thus  $P_e$  for tetryl was calculated from the U-u relation for TNT, while the  $P_e$ 's for the remaining explosives were calculated using the U-u relation for Comp B-3. The error in calculating  $P_e$ , due to an approximation of the Hugoniot, is believed to be less than 5%. The error in  $P_e$ , due to uncertainties in  $P_g$ , is also about 5%. The surface velocity  $U_a^*$ , which would be found in the absence of reaction, is taken as twice the particle velocity incident on the surface. To obtain this particle velocity, a correction must be made for the decay in the transmitted pressure due to rarefactions moving in from the direction of the gap. Although the correction is an estimate, it has been checked satisfactorily by direct measurement in those cases where no reaction occurs. For the estimate the assumption is made that the acceptor pressure decays in proportion to that which would occur if the 12.7 mm of acceptor were replaced by an equal thickness of PMMA. The proportionality factor assumed is the ratio between the shock impedances of the explosive and the PMMA. The method is illustrated in Fig. 14 for one specific experiment. The value of  $P_a^*$  thus calculated is used in the momentum equation,  $P = \rho_c U u$  to calculate the corresponding particle velocity and  $U_a^*$ .  $U_i$ ,  $U_a$ , and  $\tau$  are the direct result of measurements from experimental records.

In order to see how the free-surface motions respond to changes in the initial shock strength, axial velocities in a given experiment were computed as a function of travel distance from the recorded displacements (time intervals: 1.09 usec). The results for a series of shock strengths have been compared for several explosives. These were found to have similarities which can be illustrated by the two examples graphed in Figs. 15 and 16. In Fig. 15,  $U_i$  for cast Comp B-3 has been plotted as a function of displacement,  $x$ , for  $P_e$  varying from 10.6 to 47.0 kb. At the lowest value of  $P_e$  no chemical reaction is evident in the 10.6 kb curve. The velocity remains essentially constant at the value predicted for  $U_i^*$ . At higher incident pressures, to 32.6 kb, each velocity increases with distance after an initial jump, levels off after 10 to 20 mm of travel, and then remains relatively constant. In the range of 35.0 kb and up, the initial velocity is quite large and then decays to a relatively constant value after traveling about 50 mm. Similar results are seen for pressed Composition B-3 in Fig. 16, except that above 26 kb all velocities appear to start at the same value of 8 mm/usec. Both figures suggest that a level of shock strength exists at which the blow-off velocity is essentially constant; e.g., 33 kb for cast Comp B-3. The break point between acceleration and deceleration is at a value of  $U_i$  between 3 and 4 mm/usec. The curve in Fig. 15 at 35.8 kb suggests that transition to detonation was probably completed just as the surface was reached. One would expect that the 35.0 kb shock would have produced detonation in a slightly longer charge, whereas at 32.6 kb one cannot be sure what an increased length would do\*. At 35.8 kb a luminous air shock was formed. This may be taken as clear evidence that detonation had developed. In this report we associated the luminous shock with detonation and use this as one criterion for pin-pointing  $P_s$ .  $P_s$ , therefore, is recorded as 36 kb in Table II for this explosive.

It is desirable in reporting results to use some single value of  $U_i$  to characterize the response of the test sample to the incoming shock. The velocity chosen should reflect any possible influence due to reaction at low shock levels. The initial value at  $x=0$  has been ruled out because in the low range the maximum reaction effect does not occur immediately. The maximum velocity would be desirable, were it not so difficult to measure it at  $x=0$ , when  $U_i$  is high. We have selected the velocity at 50 mm from the surface for this report. At this point the velocity has become nearly constant for all of the explosives. It is easy to measure and is monotonely related to  $P_e$ .

\*As will be seen later, the 50% gap pressure in the NOL Standardized Gap Test is probably about 19 kb.

The time,  $\tau$ , between shock arrival and break-out of smoke or gas from the surface, provides an alternate method for characterizing the vigor of reaction. This time is obtained by inspection of the records to find both the time of shock arrival at the acceptor top surface and the time of gas break-out. In the case of TNT, the gas break-out time could not be determined with accuracy and no data are given.  $\tau$  is determined to an accuracy of about 1.0 usec.

### 3.3 Results

Values of  $U_a$ ,  $P_e$ ,  $P_g$  are reported for all experiments in Table I, A-L.  $U_a^*$  is given for comparison and  $\tau$  is reported when it could be unambiguously determined. The gap length ( $S$ ) is reported since recalibration may alter  $P_g$ . Graphs of  $\tau$  vs  $P_e$ , and  $U_a$  and  $U_a^*$  vs  $P_e$  are presented in Figs. 17-23 for all of the explosives. Inspection of the velocity-pressure plots show that the measured  $U_a$  and calculated  $U_a^*$  agree within experimental error in the range of pressures where no reaction is discernible. The point of deviation of the  $U_a$  plot from the  $U_a^*$  line pinpoints clearly the critical pressure,  $P_b$ , where internal reaction just begins to increase the blow-off velocity.  $P_b$  might, therefore, be called the shock pressure for perceptible burning or deflagration. A straight line has been drawn across the velocity graphs at a velocity of 4.5 mm/usec. In all of our records it was found that for  $U_a$  above 4.5 mm/usec, the blow-off produced a luminous air shock as it left the original surface. It is, therefore, quite clear that detonations have occurred for  $U_a$  greater than this value. For this reason the pressure at which  $U_a$  becomes equal to 4.5 mm/usec has been designated as  $P_s$ , the pressure at which luminous shock or transition to detonation just occurs. Inasmuch as  $U_a$  rises steeply at this velocity, the value of  $P_s$  is not particularly affected by our arbitrary choice of velocity.

## 4. DISCUSSION OF RESULTS

### 4.1 Shock Pressure for Initiation of Detonation

The two sets of curves,  $\tau$  vs  $P_e$  and  $U_a$  vs  $P_e$  have been constructed as a means of showing some quantitative measure of the effect of reaction. They lead to a fairly precise measure for  $P_s$ , the shock strength to initiate detonation in the experimental configuration. The test sample was deliberately made short (12.7 mm =  $d/4$ ) in order to obtain a surface effect for relatively small amounts of internal reaction. As a result, detonation in the short sample requires shock strength greater than would be needed in a much longer charge. This is what would be expected from our earlier work<sup>1</sup> on transition distance vs shock strength and this is what is found on comparing our

present results with 50% point data as shown in Table II.  $P_s$  is obtained from the  $\tau$ - $P_e$  curves as the intercept with the abscissa. This intercept is quite sharply defined.  $P_s$  is obtained from the  $U_a$ - $P_e$  data as the point where  $U_a$  becomes equal to 4.5 mm/ $\mu$ sec. As was previously stated the initial blow-off leads to a luminous shock ( $U_i \approx 6$  mm/ $\mu$ sec) when  $U_a$  exceeds 4.5 and, therefore,  $P_s$  can usually be obtained by simple comparison of a few records in which  $P_e$  is varied near its critical value. The values of  $P_s$  obtained from break-out time and velocity agree very well. The results for the various explosives are compiled in Table II. They will be discussed in Section 4.3.

#### 4.2 Shock Pressure for Initiation of Perceptible Reaction

The curves, Figs. 17-23, also permit defining a rather sharp pressure,  $P_b$ , at which evidence of reaction first becomes apparent.  $P_b$  is taken as the break point in the  $U_a$ - $P_e$  records at which  $U_a$  departs from the value it would have in the absence of reaction. The latter, termed  $U_a^*$ , is calculated with adequate precision, as previously described, to permit fixing  $P_b$  fairly precisely. The  $\tau$ - $P_e$  curves show  $\tau$  asymptotically approaching infinity as  $P_e$  approaches a limiting value presumed to be the  $P_b$  found from the  $U_a$  values. Within experimental error these two measurements of  $P_b$  are identical. Note that in these experiments we are usually able to observe the surface for about 100  $\mu$ sec, a time about 25 times greater than the transit time for the shock wave through the acceptor. When  $\tau$  is of this magnitude the pressure is essentially  $P_b$ . (The reader should not be misled by the points plotted on the  $\tau$  records at 100  $\mu$ sec with an arrow facing upward above the point. These points represent experiments in which  $U_a > U_a^*$  but no smoke breakout was observed for  $\tau < 100$   $\mu$ sec. The asymptotes in these cases were not established therefore from break-out data alone.)  $P_b$  can often be obtained from inspection of records taken at several pressures near the critical value by looking for late break-out of smoke. Fig. 6 is an example in which break-out of smoke occurs at about 20  $\mu$ sec. Though a mild surface effect is seen this experiment was still found to be about 5 kb above the critical limit. The most reliable evidence for reaction is an augmented  $U_a$ .

As shown in Figs 15 and 16, speed up of  $U_i$ , especially near the critical limit, occurs long before any break-out of smoke. This makes it quite evident that the  $\tau$ 's for smoke emergence are not induction times for reaction. Our present opinions concerning details of the surface effect will be discussed in Section 5. The values of  $P_b$  obtained are reported in Table II.

#### 4.3 Comparisons

For comparison, results of the NOL 50% gap test, which uses the same donor-gap system, are also reported where available.

NOLTR 64-53  
UNCLASSIFIED

It is seen from the Table that  $P_b/P_g$  ranges from 0.8 for pressed pentolite or tetryl to 0.24 for cast TNT. Most values are closer to 0.5. The two pressures for each explosive bracket the 50% gap test value with the mean very nearly duplicating gap-test results. Cast TNT appears to be farthest out of line in this respect. The difference here may be due to difference in sensitivity of different lots. Some difficulty has been experienced by others at NOL in reproducing both shock and impact sensitivities of different batches of TNT.

Of the four castable explosives tested in both cast and pressed form, all but pentolite show essentially the same value of  $P_b$  for the pressed and cast form. In regard to  $P_g$ , the pressed form always shows a lower pressure for transition to detonation than the cast form. This result is in agreement with evidence obtained on TNT in the wedge test, and was to be expected. There is no previous experience which would have predicted the similarity on  $P_b$  for the pressed and cast charges.

As we have noted,  $P_b$  is, in all cases, lower than the 50% gap value. Thus evidence for reaction with milder shocks than those to produce detonation has been demonstrated. We see, however, from Table II that the values of  $P_b$ , which range from 8 to 24 kb, are about 2 to 4 times greater than might have been expected from LRL results mentioned in the Introduction. The higher result can be reconciled with the LRL findings but no detailed correlation is yet possible without further experimental results. The Susan test of LRL uses a 50.8-mm diam. by 102-mm high cylinder of explosive confined in an aluminum cup. The explosive is backed by a large mass of steel. As described by Dorough<sup>3</sup>, impact on a steel plate will cause considerable crushing. The explosive will be quite markedly deformed and fractured in this stage of the impact. Ignition at the lower velocities may more likely occur when the steel body pinches the crushed HE between it and the target plate as Dorough suggests. If this is so, the impact pressure is determined almost completely by a steel on steel impact rather than by the initial shock transmitted to the explosive. Thus in the Susan tests the shock pressures which should probably be used are 2 to 4 times greater than our initial estimate based on HE impacting on steel. Secondly, the deformed and fractured explosive may be more sensitive to shock. Finally, the impulse due to the large moving steel block is considerably greater than the impulse available at comparable pressure levels in our modified gap test experiment. The increased duration of the pressure pulse should act to produce more reaction at lower pressures. Work to be reported later by one of us has shown that acceptors fully surrounded by water do react at much lower pressure levels than are reported here.

## 5. GENERAL DISCUSSION

When the present experiments were begun the expectation was that internal burning, at shock input levels below the critical value for transition to detonation, would be detected largely by a time-delayed evolution of deflagration products from the free surface. Perhaps the most significant result of these experiments is the unexpected finding that long before any product gases or smoke appeared the effect of reaction became evident by an observed increase in surface velocity. At low shock amplitude this increase is a function of time. As a consequence of this effect, it has become possible to detect a relatively small amount of reaction.

The appearance of the dome-like surface motion of the acceptor is found to resemble quite closely the surface effect from an explosion in shallow water. About the time this work began Goertner<sup>13</sup> acquainted the authors with some of his high-speed photographs of explosions of one-pound spheres of TNT detonated in water. The center of the sphere and the bottom of a pool of water were located 16.5 cm below the water surface. On detonating the charge, a dome-shaped spray of water was shown to form. The mean axial velocity of the "spray dome" was 0.4 mm/usec. Another underwater experiment on a much smaller scale also is reported by Goertner<sup>13</sup>. In this instance a 0.3-g charge of lead azide was detonated under 12.7 mm of water, the bottom of the container being made of PMMA. The spray-dome velocity was comparable to that obtained in the large-scale experiment.

By comparison with these shallow water explosions, one quite reasonably could attribute the blow-off in our explosive experiments, at an excess surface velocity of 0.4 mm/usec, to an explosion of 0.2-0.5 g of acceptor material. (A total of 41-48 g of explosive is contained in the acceptor.) The explosion is assumed to occur in the vicinity of the PMMA-acceptor boundary. An incoming shock having an amplitude only slightly greater than  $P_b$  would be enough to cause an excess velocity of 0.4 mm/usec. We therefore envision our result as being due to an internal explosion followed by a spray-dome type of expulsion of explosive particles (gas at higher amplitude). As a preliminary estimate we would guess that our detection limit for the amount of reacted material would be 0.1 g.

In continuance of this line of reasoning the speed-up of surface velocities, plotted in Figs. 15 and 16 at pressures just above  $P_b$ , can be attributed to a delay in the effect of internal reaction on the surface motion. At higher shock amplitudes the internal reaction develops fast enough to influence the surface motion immediately on arrival of the first

shock. In addition, material closer to the free surface is included in the reaction. At still higher amplitude the augmented reaction must cause still greater energy release from explosive nearer the free surface until, as usually argued, shock-to-detonation transition takes place. It would be of interest to check on the spray-dome idea by obtaining microflash X-ray pictures of the acceptor about 20 usec after blow-off begins. Any gas pocket formed should be apparent in flash radiographs.

The pressures,  $P_g$ , reported here as pressures for transition to detonation can be related to other work with wedges or longer cylinders. Considering the likely difference in pressure-time curves in comparison with the NOL wedge experiment, the pressures found for the 12.7 mm transition distance (S) are in reasonable agreement with pressure vs S data discussed in Reference 1.

In the course of the investigation a limited number of other experimental conditions were explored. These included the use of longer acceptors, addition of a steel case around the acceptor, and imbedding of a small charge (12.7 mm diam x 12.7 mm high) in a collar of Saran\*. Details will be given in a later report. Results of experiments in which the acceptor is submerged in water and shocked are being reported in a paper for the Fourth Symposium on Detonation<sup>4</sup>.

---

\* Saran, registered trademark for vinylidene chloride (density = 1.65 g/cm<sup>3</sup>), Dow Chemical Co., Midland, Michigan.

6. REFERENCES

1. S. J. Jacobs, T. P. Liddiard, Jr. and B. E. Drimmer, "The Shock-to-Detonation Transition in Solid Explosives", 9th International Symposium on Combustion, Academic Press, N.Y. (1963), p. 517-526. (A fairly complete bibliography of earlier work is given on p. 526.)
2. I. Jaffe, R. Beauregard, and A. Amster, "Determination of Shock Pressure Required to Initiate Detonation of an Acceptor in a Shock Sensitivity Test", ARS Jour. 32, 22(1962).
3. G. D. Dorough, L. G. Green, E. James, Jr., and D. T. Gray, "Ignition of Explosives by Low Velocity Impact", Int'l Conference on Sensitivity and Hazards of Explosives, London 1-3 Oct 1963. Explosives Research & Development Laboratory, Waltham Abbey, Essex, England.
4. R. J. Eichelberger and M. Sultanoff, "Sympathetic Detonation and Initiation by Impact", Proc. Roy. Soc. A246, 274 (1958).
5. R. B. Clay, M. A. Cook, T. Keyes, O. K. Shope, and L. L. Udy, "Ionization in the Shock Initiation of Detonation", 3rd Symposium on Detonation, Princeton Univ., 26-28 Sep 1960; ONR Symp. Rpt. ACR-52, Vol. 1, p. 150.
6. H. S. Napadensky, R. H. Stresau, and J. Savitt, "The Behavior of Explosives at Impulsively Induced High Rates of Strain", *ibid.* Vol. 2, p. 420.
7. T. P. Liddiard, Jr. and D. Price, "Recalibration of the Standard Card-Gap Test", NOLTR 65-43 (in publication).
8. S. J. Jacobs, J. D. McLanahan, Jr., and E. C. Whitman, "A High-Speed Focal Plane Shutter Framing Camera", Jour. SMPTE 72, 12, p.923 (1963). Also Proc. of the 6th Int'l Congress on High Speed Photography, The Hague, Netherlands, Tjeenk Willink-Haarlem (1963), p. 57.
9. T. P. Liddiard, Jr., B. E. Drimmer, and S. J. Jacobs, "Applications of the High-Speed Focal-Plane Shutter Camera to Explosives Research", *ibid.* Jour. SMPTE, p. 57, and Proc. 6th Congress, p. 497.
10. Z. Pressman, "High Intensity Explosive Light Source", Proc. of the 5th Int'l Congress on High Speed Photography, Soc. Mot. Pict. & Telev. Engr., N. Y. (1962) p.56.
11. T. P. Liddiard, Jr., "The Unreacted Shock Hugoniot for TNT and Composition B-3", Int'l Conference on Sensitivity and Hazards of Explosives, London, Oct 1963.
12. N. L. Coleburn and T. P. Liddiard, Jr., "The Unreacted Hugoniot Equations-of-State of Several Explosives". In preprint of the 4th Symposium on Detonation, Oct 1965.
13. J. F. Goertner, "Pressure Waves in the Air above a Shallow Underwater Explosion: An Approximate Calculation by the Method of Characteristics", Master of Science Thesis, Univ. of Maryland (Dec 1964). To be published as NOLTR 65-31.
14. T. P. Liddiard, Jr., "The Initiation of Burning in High Explosives by Shock Waves", in preprint of the 4th Symposium on Detonation, Oct 1965.

TABLE I

ACCEPTOR VELOCITY ( $U_a$ ) AND BREAK-OUT TIME ( $\tau$ ) FOR SEVERAL EXPLOSIVES AT VARIOUS ENTERING STRESSES ( $P_e$ ) WHICH CORRESPOND TO THE GAP LENGTH ( $S$ ) AND GAP STRESS ( $P_g$ ).  $U_a^*$  IS THE CALCULATED ACCEPTOR VELOCITY WITHOUT CHEMICAL REACTION.

Material	Shot No.	S (mm)	$P_g$ (kb)	$P_e$ (kb)	$U_a$ (mm/ $\mu$ sec)	$U_a^*$ (mm/ $\mu$ sec)	$\tau$ ( $\mu$ sec)
A. Tetryl <sup>a</sup> Density = 1.648 g/cm <sup>3</sup> Lot No. X 102 (CH 5291)	90B	76.9	7.9	8.7	0.25	0.31	—
	90T	71.1	8.9	9.9	0.30	—	—
	93B	63.5	11.1	12.5	0.37	0.39	>100
	92B	58.4	13.3	15.1	0.88	—	14
	93T	54.6	15.2	17.4	2.59	—	1-2
	92T	51.3	17.1	19.8	5.16	0.50	0
B. TNT, pressed Density = 1.619 g/cm <sup>3</sup> Lot No. X 412 (CH 5294)	63B	48.3	19.2	22.4	0.63	0.58	b
	68B	41.1	26.6	31.2	1.85	0.70	—
	64B	35.5	34.9	41.1	3.02	0.84	—
	70B	32.5	39.4	46.2	3.81	0.93	—
	67B	29.0	44.0	51.8	4.59	1.06	—
70T	26.2	48.2	57.0	5.01	1.18	—	
C. TNT, cast Density = 1.615 g/cm <sup>3</sup> Lot No. X 412 (CH 5307)	63T	48.3	19.2	22.4	0.65	0.58	b
	64T	35.5	34.9	41.1	1.12	0.84	—
	67T	34.0	37.0	43.4	1.23	0.88	—
	68T	29.0	44.0	51.8	1.68	1.06	—
	69T	17.0	65.0	77.1	3.07	1.57	—
D. Pentolite, pressed, density = 1.667 g/cm <sup>3</sup> Lot Nos: PETN X 321 TNT X 412 (CH 5298)	113B	71.9	8.8	10.2	0.30	0.32	>100
	114B	69.9	9.2	10.7	0.46	—	35
	128B	67.8	9.7	11.4	1.48	—	24
	111B	66.0	10.2	11.9	1.75	—	14
	120T	64.8	10.7	12.5	1.91	0.36	8
	120B	64.1	10.9	12.8	2.01	—	8
	128T	62.3	11.5	13.6	2.50	—	2-3
	133B	60.7	12.1	14.2	4.50	0.39	0
E. Pentolite, cast density = 1.640 g/cm <sup>3</sup> Lot Nos. same as above. (CH 5328)	139B	81.4	7.2	8.4	0.19	0.27	>100
	142B	78.8	7.6	8.9	1.38	—	28
	139T	75.2	8.1	9.5	1.69	—	14
	113T	71.9	8.7	10.1	1.75	—	10
	114T	69.9	9.2	10.7	1.79	—	8
	119T	66.0	10.2	11.9	2.04	—	5
	140T	62.3	11.5	13.4	2.46	—	2
	140B	60.7	12.1	14.1	2.62	0.39	1
141B	59.1	12.9	15.1	2.72	—	<1	
F. Comp. B-3, pressed density = 1.715 g/cm <sup>3</sup> Lot. No. X 276 (CH 5254)	57B	66.7	10.0	12.0	0.35	0.34	—
	52B	64.2	10.8	12.9	0.35	—	—
	50B	62.3	11.4	13.6	0.44	—	>100
	47B	55.1	14.9	18.0	1.58	—	20
	46B	47.8	19.6	24.0	2.67	0.52	5
	53B	46.2	21.0	25.7	4.70	—	0
	48B	44.5	22.6	27.7	5.25	—	0
	56B	43.0	24.2	29.8	5.13	—	0
	49B	39.8	28.5	35.0	5.79	0.69	0
	61B	71.7	8.9	10.6	0.26	0.31	—
G. Comp. B-3, cast density = 1.712 g/cm <sup>3</sup> Lot. No. X 276 (CH 5263)	57T	61.0	12.0	14.3	0.42	—	—
	52T	57.6	13.5	16.3	0.61	0.40	70
	50T	54.9	15.0	18.1	0.93	—	39
	47T	51.6	17.0	20.7	1.22	—	31
	46T	47.8	19.6	24.0	1.75	0.52	13
	48T	41.1	26.6	32.6	3.10	—	2
	53T	39.8	28.5	35.0	3.98	0.69	0
	56T	39.3	29.1	35.8	4.70	—	0
	49T	33.3	38.1	47.0	5.50	0.86	0

CONTINUED

TABLE 1 (cont'd)

Material	Shot No.	S (mm)	P <sub>g</sub> (kb)	P <sub>e</sub> (kb)	U <sub>a</sub> (mm/usec)	U <sub>a</sub> <sup>*</sup> (mm/usec)	τ (usec)
H. 60/40 Cyclotol pressed, density = 1.700 g/cm <sup>3</sup> Lot Nos: RDX - X 334 TNT - X 412 (CH 5292)	134B	64.7	10.6	12.6	0.36	c	91
	131B	60.7	12.0	14.5	1.32	—	27
	131T	56.6	14.1	17.1	1.55	—	15
	116B	53.3	15.9	19.3	1.70	—	15
	133T	47.2	20.1	24.6	1.97	—	9
	142T	44.7	22.3	27.4	3.57	—	1
	137B	42.3	25.0	30.6	5.00	—	0
I. 60/40 Cyclotol cast, density = 1.697 g/cm <sup>3</sup> Lot Nos: same as above. (CH 5306)	134T	60.7	12.0	14.5	0.40	c	>100
	135B	56.6	14.1	17.1	0.57	—	40
	116T	53.3	15.9	19.3	0.81	—	37
	132B	50.0	18.0	21.8	1.20	—	11
	132T	47.2	20.1	24.6	1.35	—	7
	135T	41.1	26.6	32.6	1.85	—	4
	138T	38.0	31.0	38.0	2.38	—	1
	138B	36.1	33.9	41.8	2.67	—	<1
J. PBX 9404-03 <sup>d</sup> Density = 1.832g/cm <sup>3</sup> (CH 5296)	81B	62.7	11.3	13.6	0.33	0.36	—
	77B	59.0	12.8	15.7	0.33	—	—
	81T	57.1	13.8	16.8	1.11	0.40	26
	79B	54.4	15.3	18.8	1.68	—	15
	76B	49.8	18.1	22.7	2.31	0.48	7
	79T	46.8	20.4	24.7	2.62	—	6
	74B	43.8	23.3	29.3	2.99	0.58	5
	94B	40.7	27.1	34.2	4.53	—	2
	95B	38.0	30.5	38.4	5.70	0.71	0
K. LX-04-0 <sup>e</sup> Density = 1.857 g/cm <sup>3</sup> (CH 5212)	39B	48.0	19.4	24.6	0.63	0.50	44
	40T	42.2	25.1	31.8	1.70	0.61	13
	42B	38.0	30.5	38.6	4.04	0.70	3.5
	41T	37.0	32.5	41.2	4.72	—	0
	38T	31.8	40.2	51.4	5.72	0.88	0
L. LX-04-1 <sup>f</sup> Density = 1.862 g/cm <sup>3</sup> (CH 5295)	77T	50.1	17.9	22.8	0.47	0.47	—
	76T	45.8	21.4	27.2	1.14	—	20
	74T	40.1	28.0	35.5	1.85	0.65	8
	95T	36.0	34.1	43.4	4.67	—	0
	94T	34.3	36.6	46.6	5.21	0.80	0

<sup>a</sup> Yellow crystals, ungraphited.

<sup>b</sup> Values of τ cannot be determined since there is insufficient contrast between the gas and the surrounding unburned explosive.

<sup>c</sup> For these calculations 60/40 Cyclotol is considered to be the same as Comp B-3.

<sup>d</sup> PBX 9404-03 - HMX/nitrocellulose/tris (β-chloroethyl) phosphate in the weight percentages of 94/3/3. The "03" denotes a bimodal particle size distribution of the HMX.

<sup>e</sup> LX-04-0 and LX-04-1 = HMX/Viton A; 85/15. The "-0" and "-1" denote certain specifications, e.g., particle size, of the HMX. Viton A is a registered trademark for a fluoro elastomer made by duPont.

TABLE II

THE THRESHOLDS OF BURNING ( $P_b$ ) AND DETONATION ( $P_s$ ) AND THE 50% FIRING PRESSURES (P) OF THE STANDARD GAP TEST USING CONFINED ACCEPTORS.

EXPLOSIVE	MOD. GAP TEST			STND. GAP TEST	
	% TMD	$P_b$ (kb)	$P_s$ (kb)	% TMD	P (kb)
50/50 Pentolite (p)	97.5	11	14	97.3	10
50/50 Pentolite (c)	95.9	8	[18]	97.6	11
COMP B-3 (p)	98.6	14	26	—	—
COMP B-3 (c)	98.4	14	36	98.6	19
60/40 Cyclotol (p)	97.8	13	27	—	—
60/40 Cyclotol (c)	97.6	15	47	—	—
COMP B, ordinary (p)	—	—	—	96.7	16
COMP B, ordinary (c)	—	—	—	99.1	21
TNT (p)	97.9	22	50	96.9	24
TNT (c)	97.6	22	[50]	97.5	44
Tetryl*	95.3	14	18	94.9	14
PBX 9404**	98.2	16	34	94.9	16
LX-04-0	97.8	23	39	97.5	32
LX-04-1	98.1	23	43	—	—

TMD = Theoretical Maximum Density.

(p) = Pressed and (c) = Cast.

[ ] = Extrapolated Value.

\*Ungraphited in Mod. Gap Test; 1/2% graphite in Stnd. Test.

\*\*9404-03 in Mod. Test; particle size unknown in Stnd. Test.

NOTE: All explosives used in the Mod. Gap experiments, except the plastic-bonded materials, were sieved through 70 onto 100 mesh screen. Except for Comp B-3 (X 2/6), TNT (X 412), and LX-04-0, the explosives used in the Mod. Tests were not from the same lot used in the Stnd. Tests.

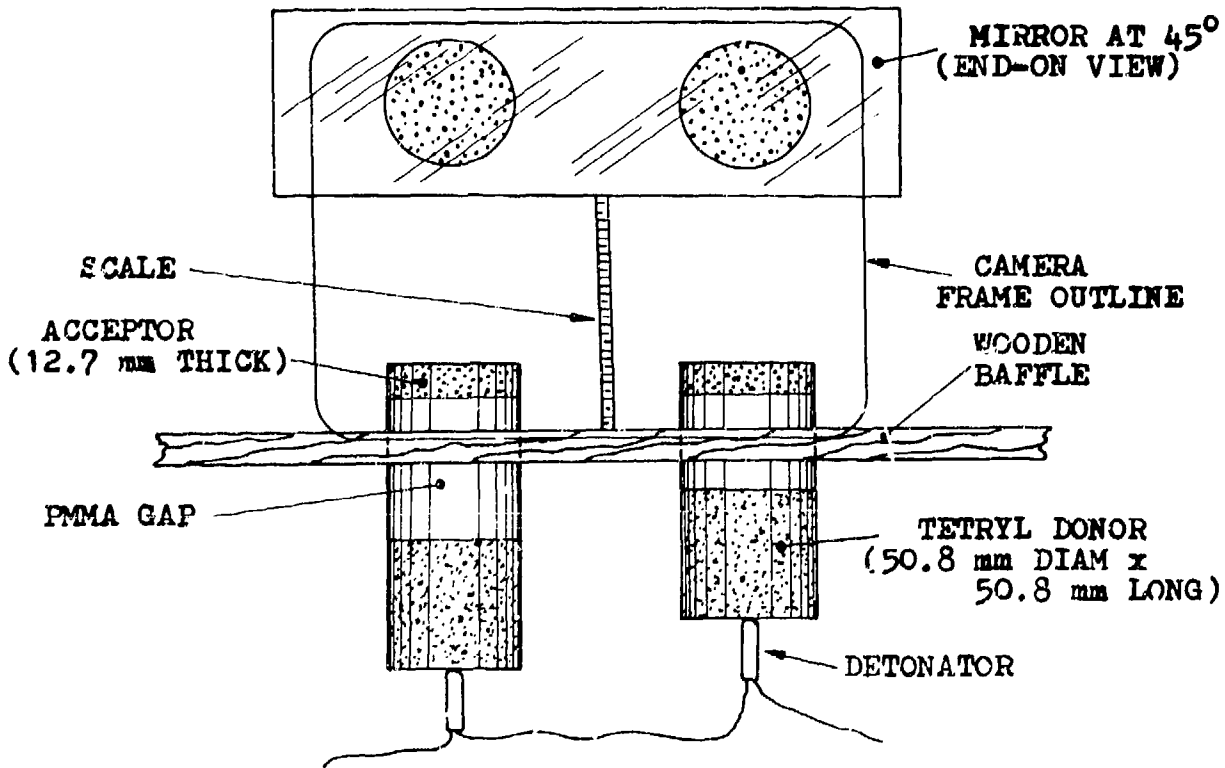


FIG. 1. THE MODIFIED GAP-TEST ARRANGEMENT

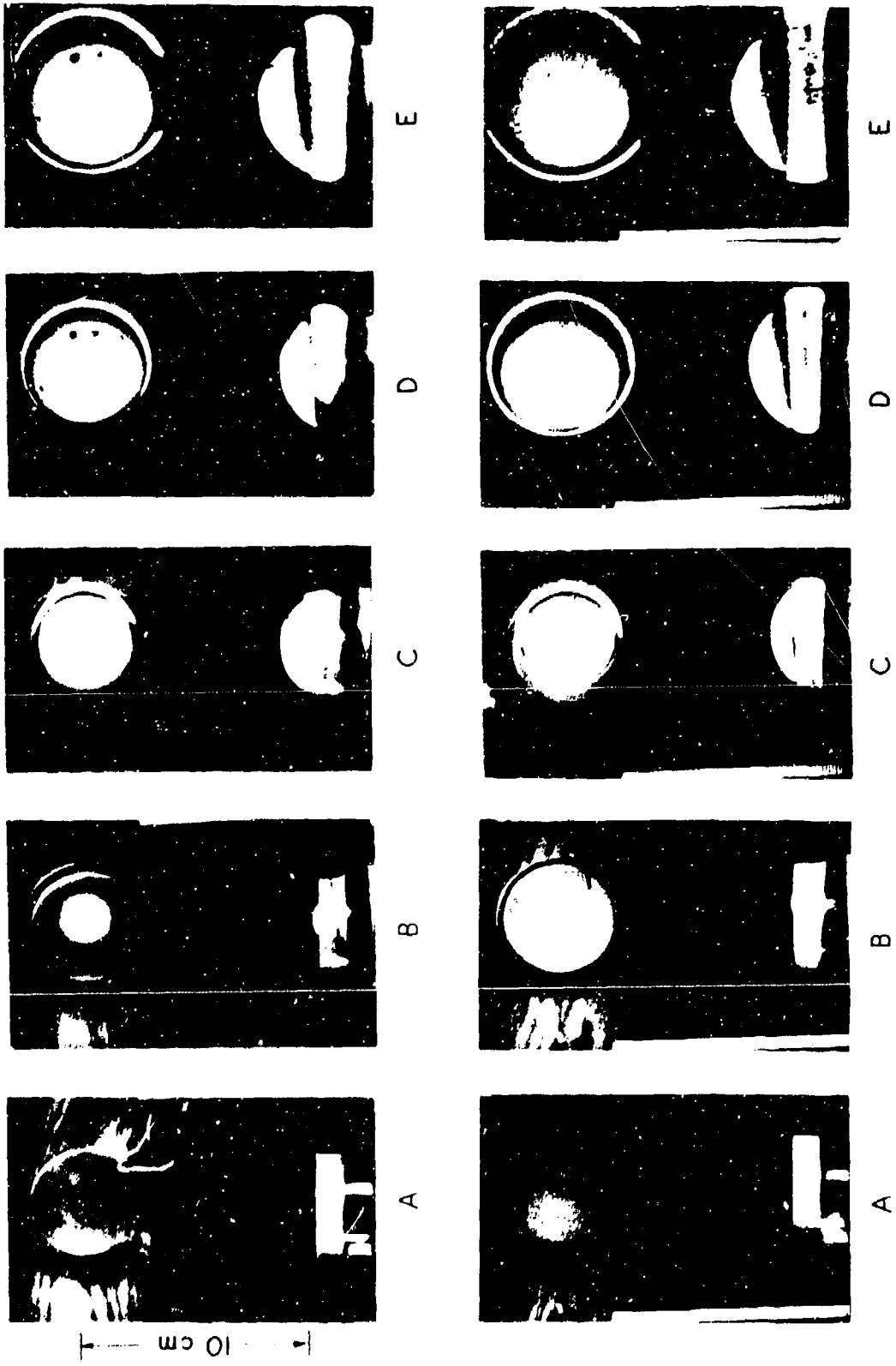


FIG. 2. DETONATION PRODUCED IN CAST COMP B-3 (UPPER ROW) AT  $P_8 = 47.0$  kb AND IN PRESSED COMP B-3 (LOWER ROW) AT  $P_8 = 35.0$  kb. [INTERFRAME TIME (BOTH ROWS) = 1.09  $\mu$ sec; EXPOSURE TIME (FOCAL PLANE SHUTTER) = 0.065  $\mu$ sec. SHUTTER MOVES FROM LEFT TO RIGHT. SEE TEXT FOR EXPLANATION OF CAMERA AND RESULTING RECORDS. PICTURES SHOWN HERE COVER ONLY ONE-HALF OF THE TOTAL FRAME AREA.]

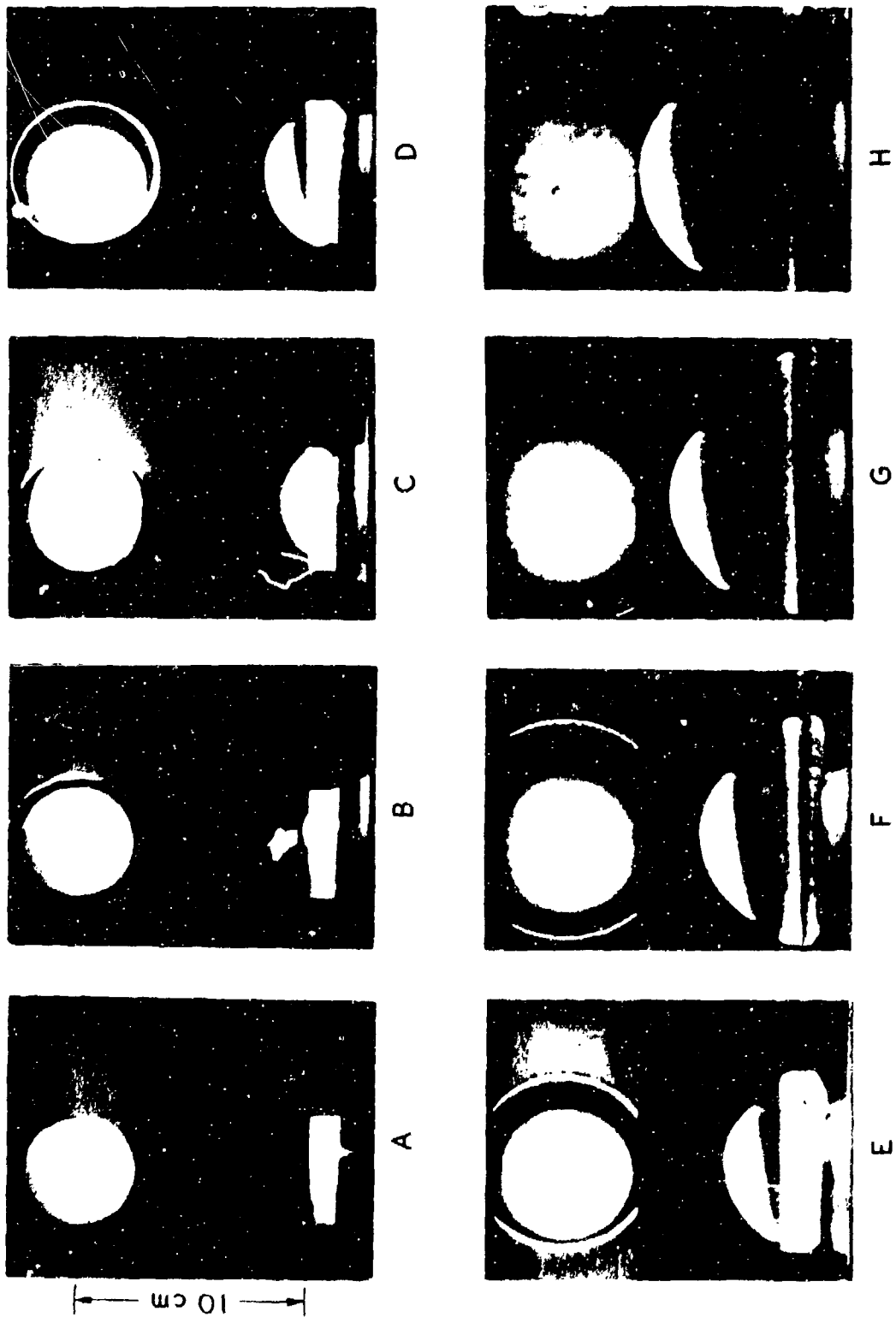


FIG. 3. FULL DETONATION PRODUCED IN LX-04-0 AT  $P = 51.4$  kb. [INTERFRAME TIME = 1.09  $\mu$ sec. PICTURES HERE COVER THREE-FIFTHS OF THE TOTAL FRAME AREA. OTHER CONDITIONS AS IN FIG. 2.]

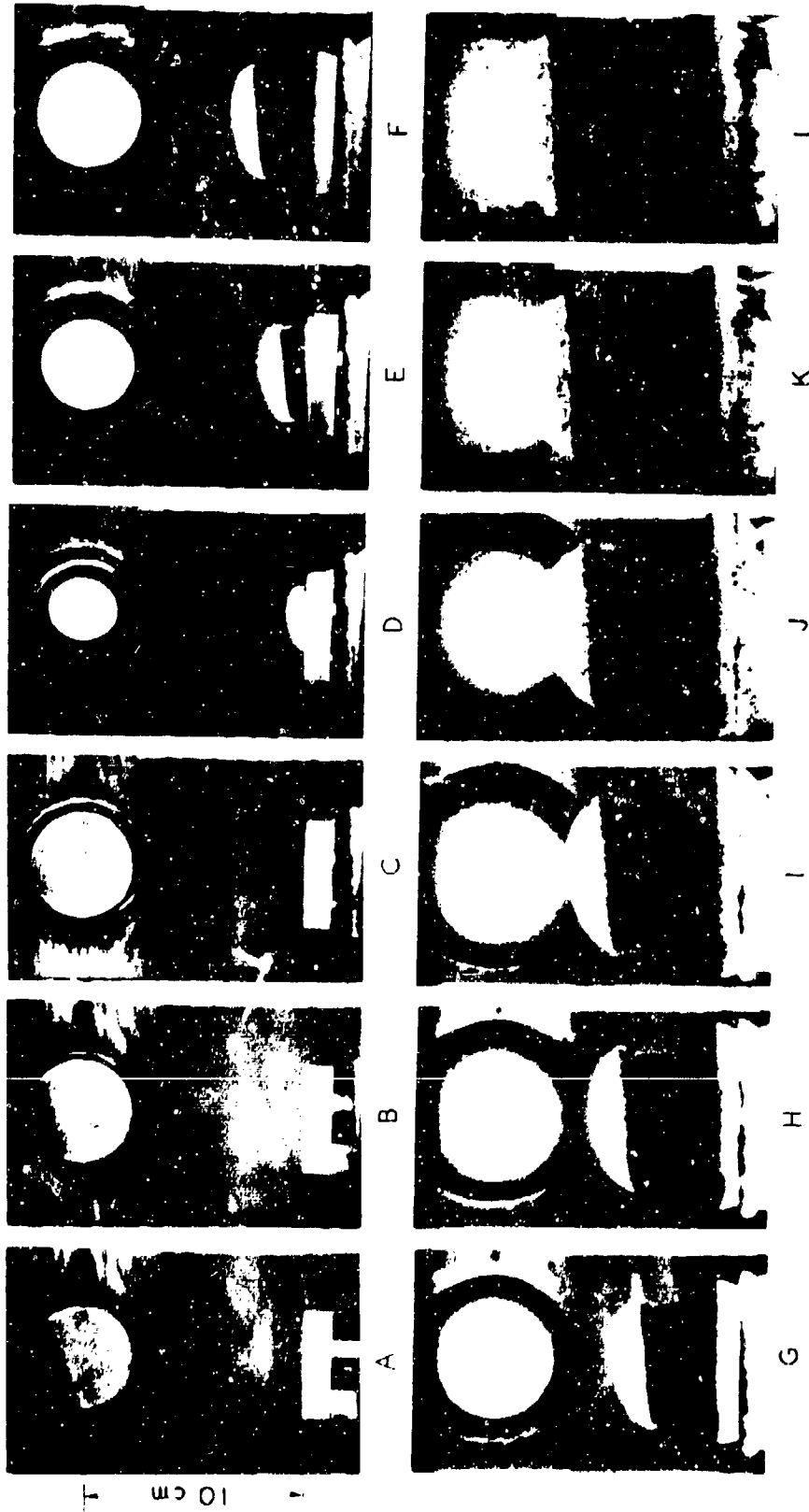


FIG. 4. AN ALMOST COMPLETELY DETONATED TNT (PRESSED) ACCEPTOR AT  $P_a = 57.0$  kb.  
[INTERFRAME TIME = 2.18  $\mu$ sec. OTHER CONDITIONS AS IN FIG. 2.]

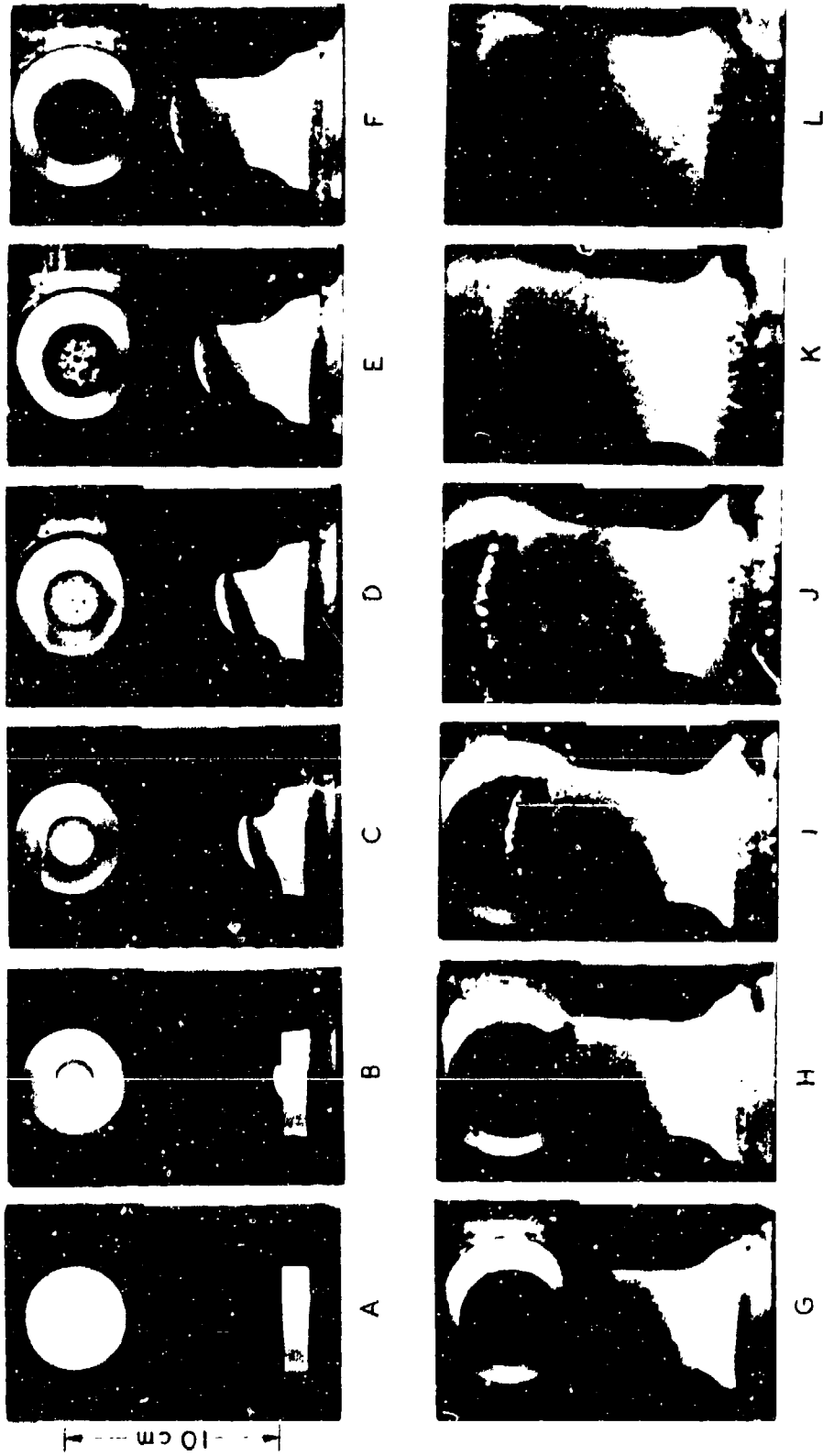


FIG. 5. PARTIAL DETONATION IN LX-04-O AT  $P_0 = 41.2$  kb. [2.18  $\mu$ sec BETWEEN FRAMES IN THE SEQUENCE A TO G; 4.36  $\mu$ sec BETWEEN FRAMES FROM G TO L. OTHER CONDITIONS AS IN FIG. 2.]

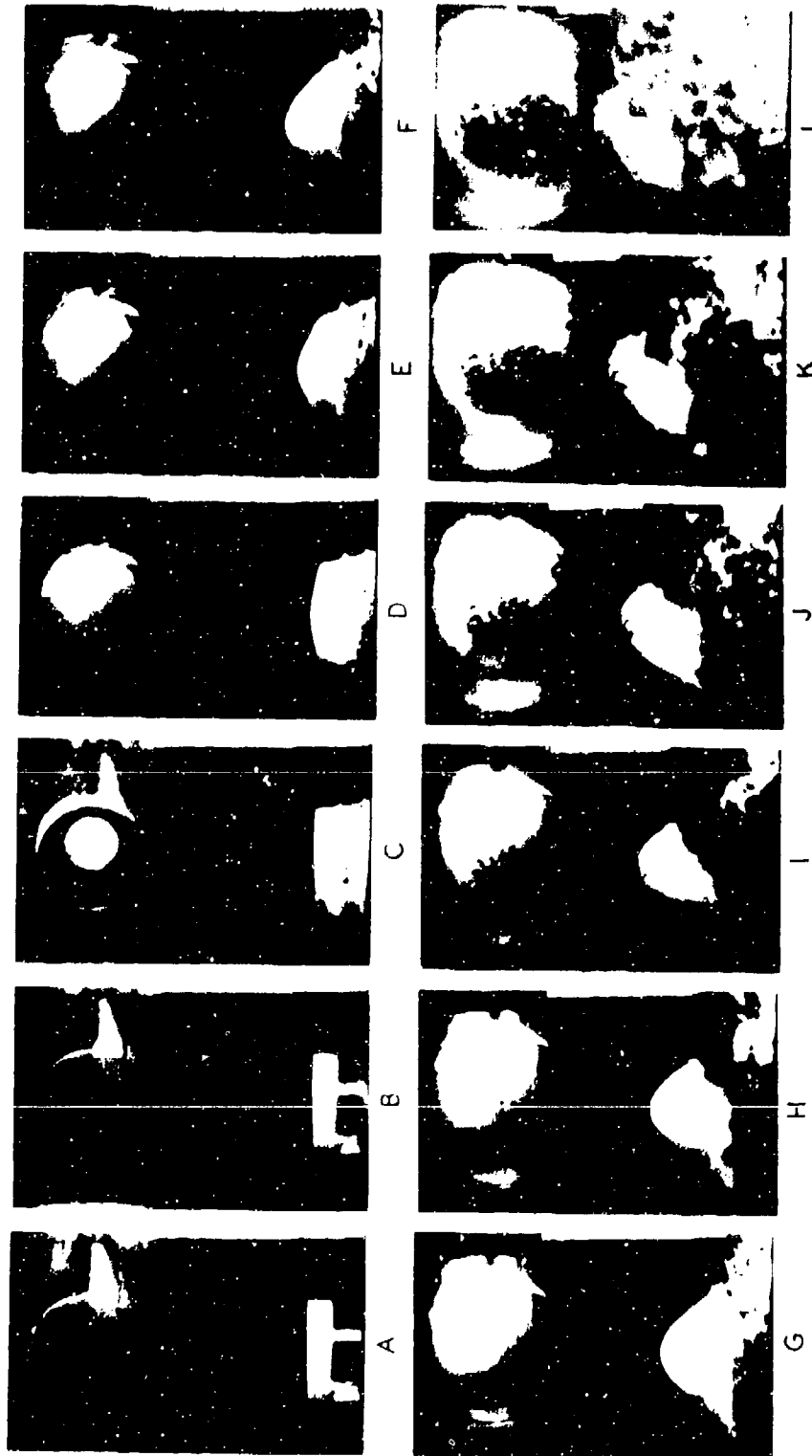


FIG. 6. MODERATE BURNING PRODUCED IN CAST COMP B-3 AT  $P_0 = 20.7$  kb.  
[INTERFRAME TIME = 6.55 msec. OTHER CONDITIONS AS IN FIG. 2.]

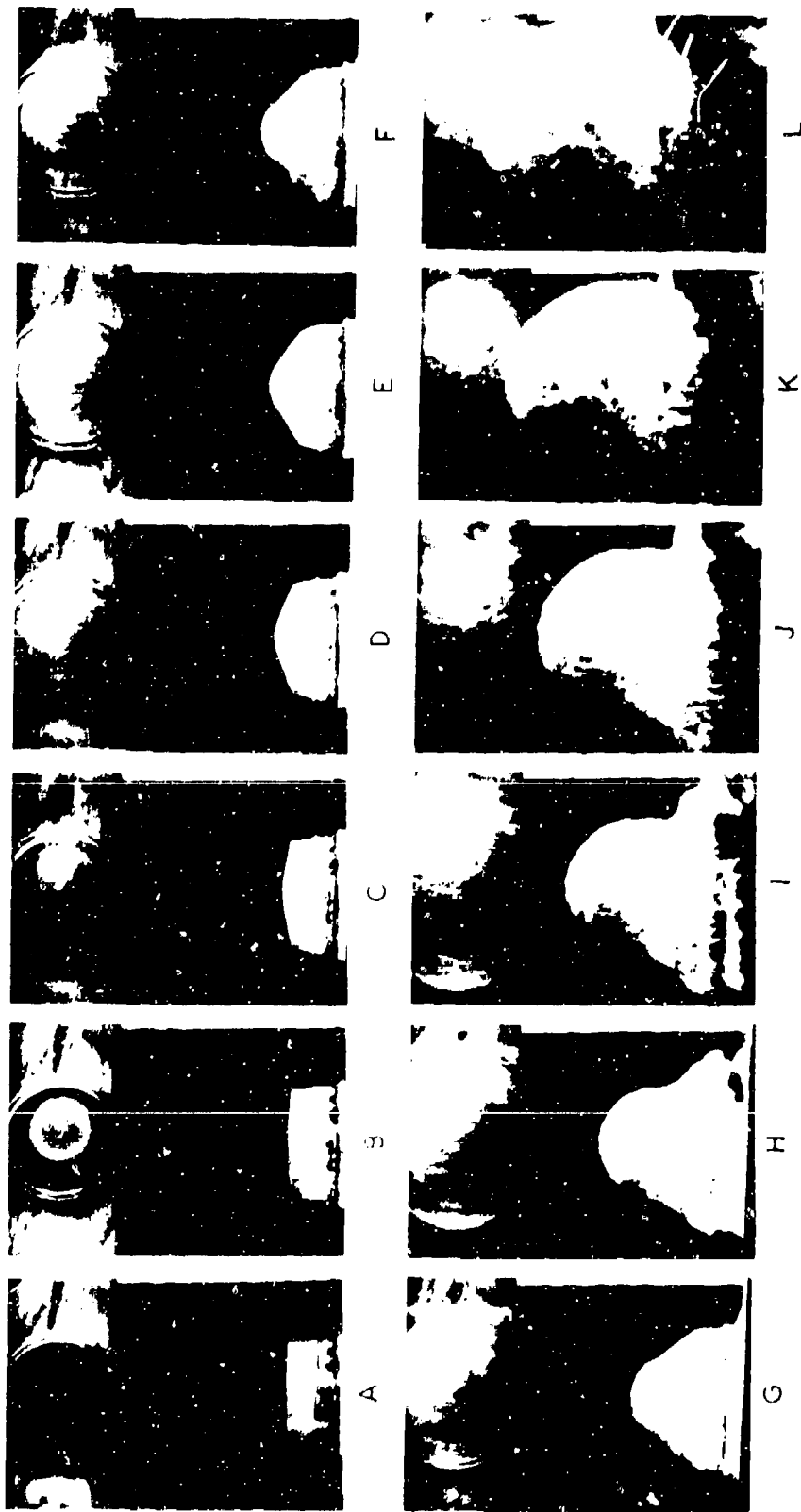


FIG. 7. VIGOROUS BURNING IN PBX 9404 PRODUCED AT  $P_0 = 24.7$  kb. [2.18  $\mu$ sec BETWEEN FRAMES IN THE SEQUENCE A TO G; 6.53  $\mu$ sec BETWEEN FRAME FROM G TO L. OTHER CONDITIONS AS IN FIG. 2.]

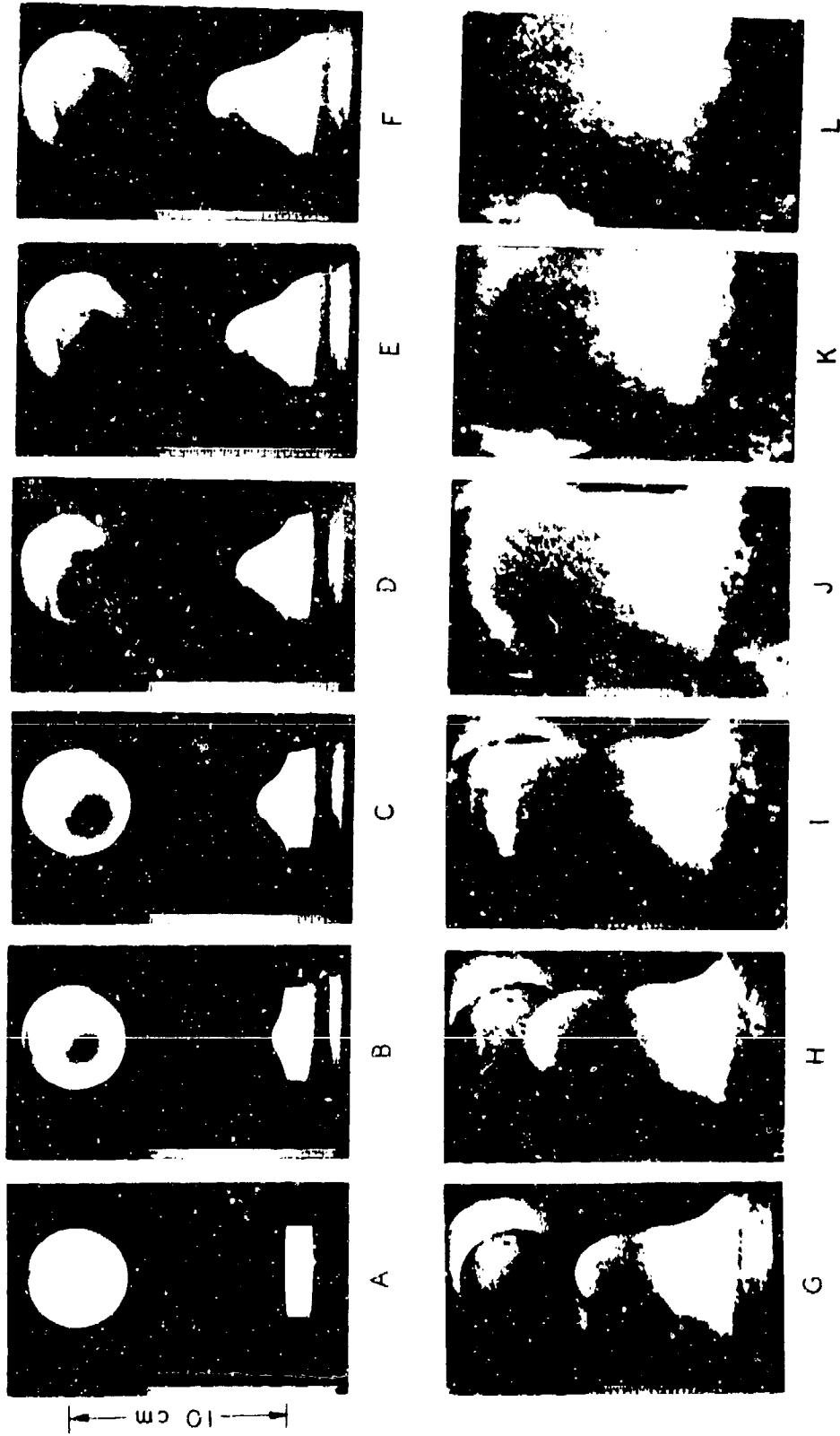


FIG. 8. VIOLENT BURNING PRODUCED IN LX-04-0 AT  $P_0 = 38.6$  kb. [2.18  $\mu$ sec BETWEEN FRAMES A TO F; 6.53  $\mu$ sec BETWEEN FRAMES FROM F TO L. OTHER CONDITIONS AS IN FIG. 2.]

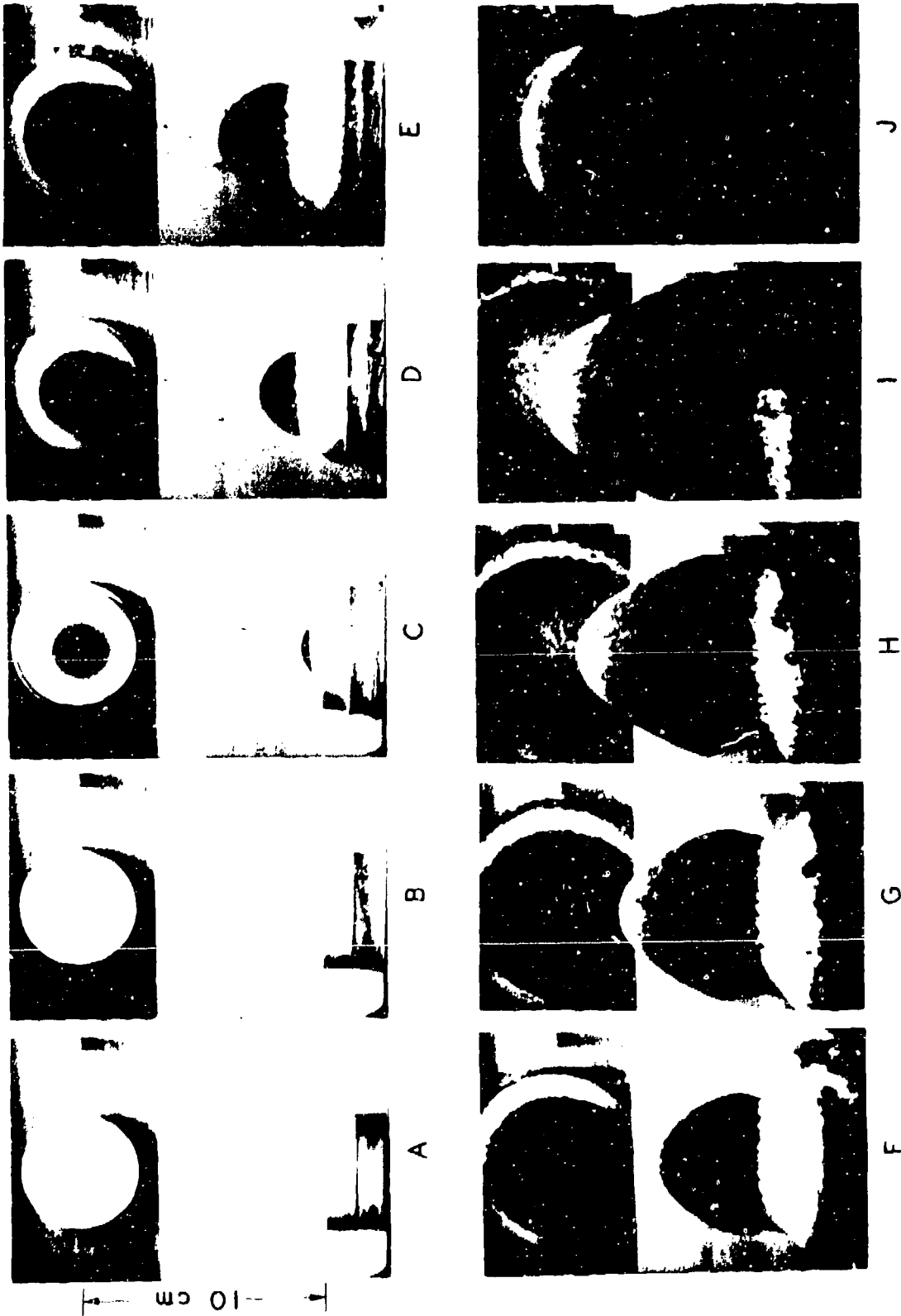


FIG. 9. VIGOROUS BURNING IN TETRYL AT  $P_0 = 17.4$  kb. [6.53  $\mu$ sec BETWEEN ALL FRAMES FROM B TO J. OTHER CONDITIONS AS IN FIG. 2.]

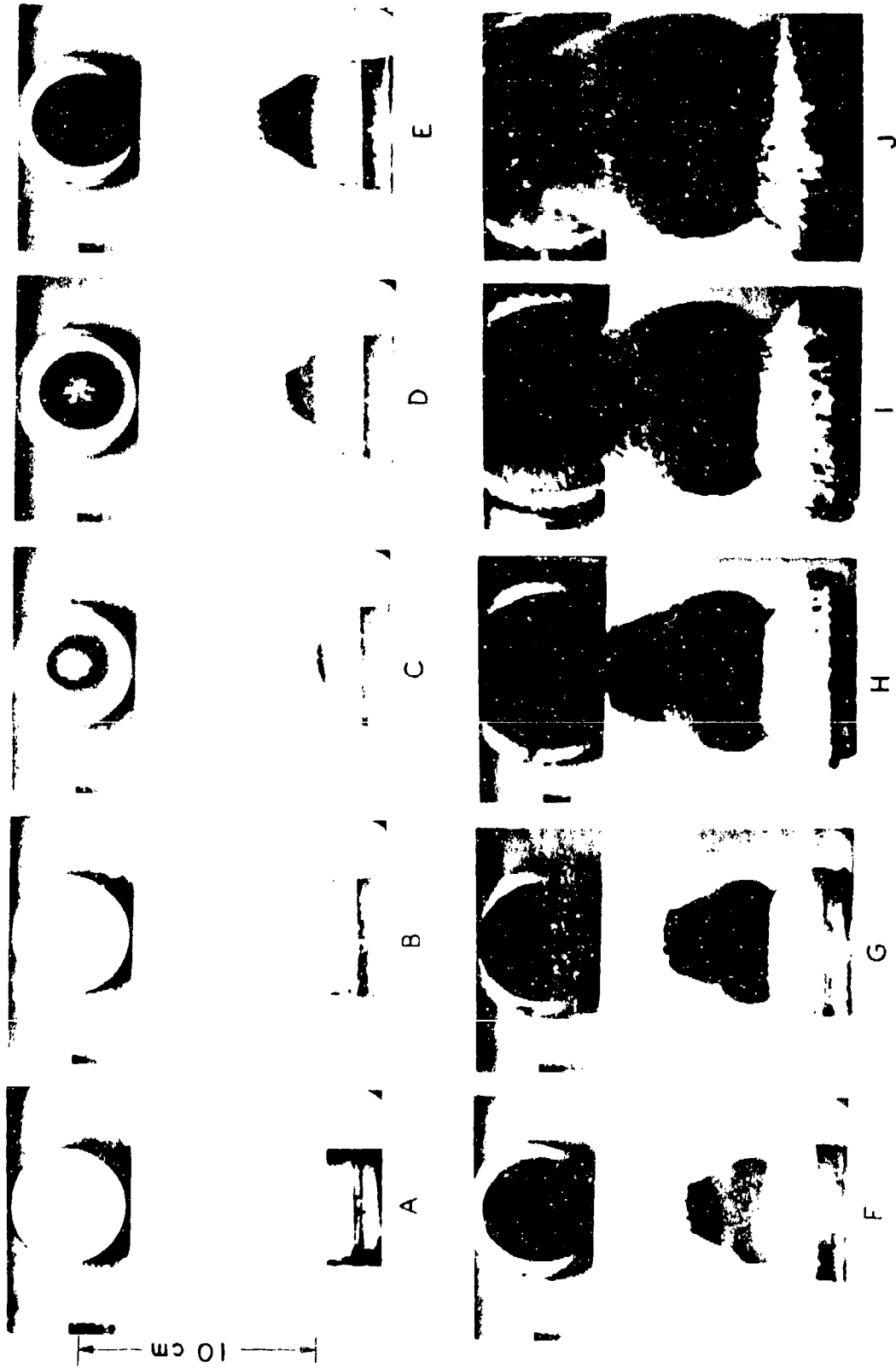


FIG. 10. A "PARTIAL DETONATION" IN PRESSED PENTOLITE AT  $P_e = 14.1$  kb. [2.18  $\mu$ sec BETWEEN FRAMES FROM B TO G; 6.53  $\mu$ sec BETWEEN FRAMES FROM G TO J. OTHER CONDITIONS AS IN FIG. 2.]

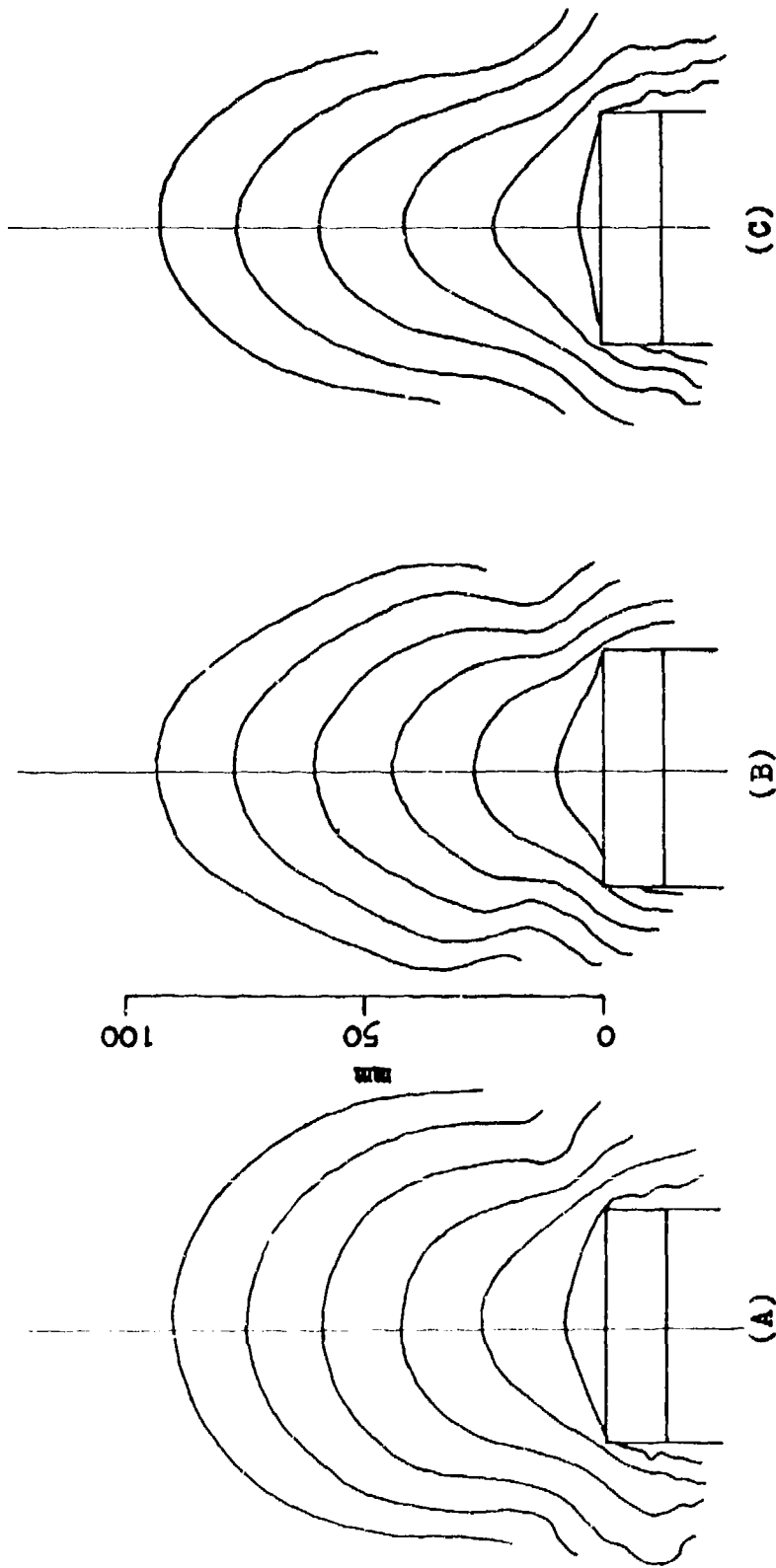


FIG. 11. PROFILES OF VIGOROUSLY REACTING ACCEPTORS: (A) PBX 9404 AT  $P_{0.5} = 24.7$  kb, (B) TETRYL AT  $P_{0.5} = 17.4$  kb, AND (C) PRESSED COMP B-3 AT  $P_{0.5} = 24.0$  kb.  $U_a$  IS 2.50 TO 2.60 mm/ $\mu$ sec IN ALL THREE CASES; 6.53  $\mu$ sec BETWEEN SUCCESSIVE OUTLINES.]

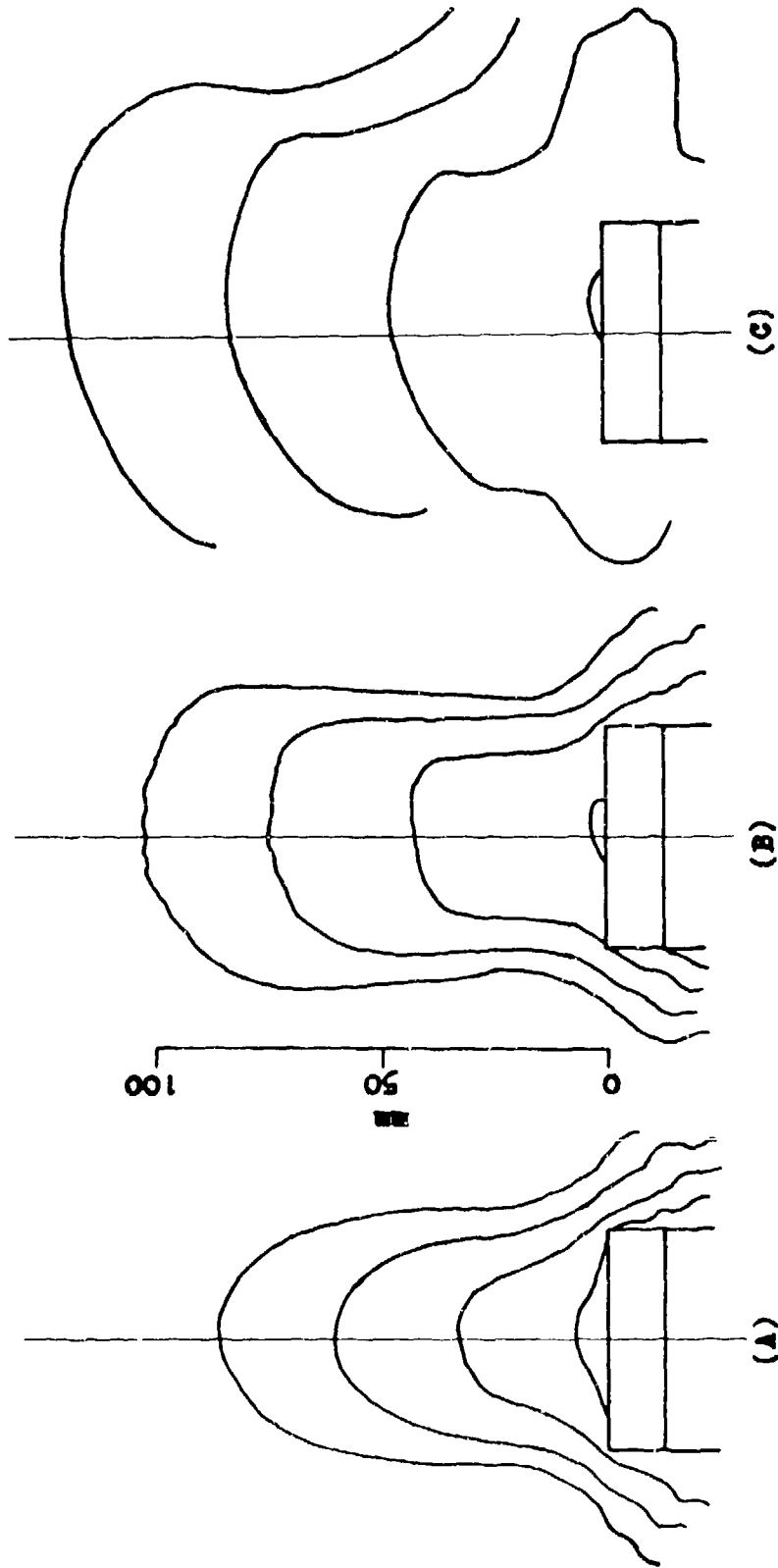


FIG. 12. PROFILES OF REACTING LX-04-O ACCEPTORS: (A) VIOLENT REACTION AT  $P_0 = 38.6$  kb, (B) "PARTIAL DETONATION" AT  $P_0 = 41.2$  kb, (C) FULL DETONATION AT  $P_0 = 51.4$  kb. [6.53  $\mu$ sec BETWEEN SUCCESSIVE OUTLINES.]

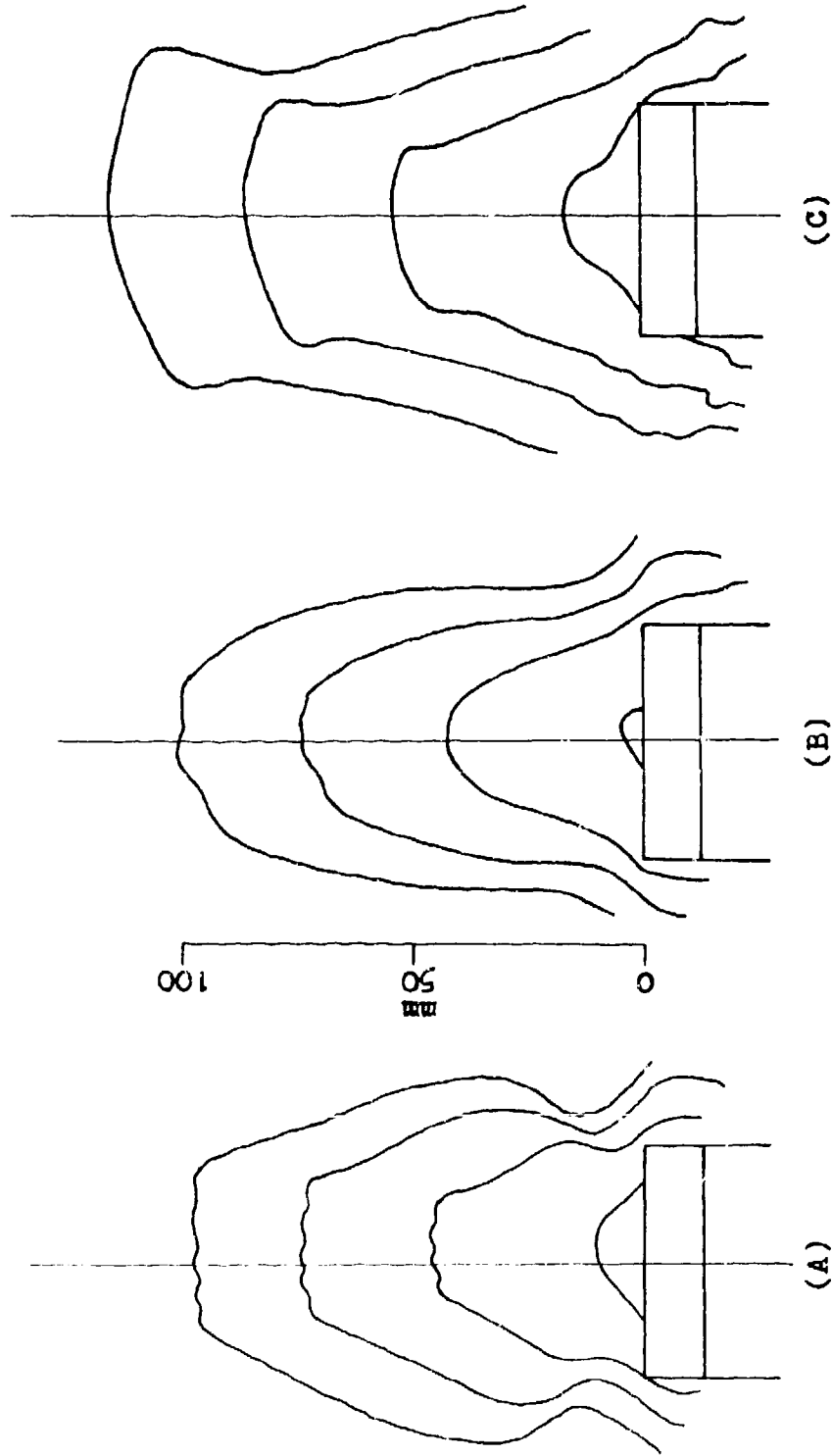


FIG. 13. PROFILES OF "PARTIALLY DETONATING" ACCEPTORS: (A) PRESSED PENTOLITE AT  $P_e = 14.1$  kb, (B) PRESSED COMP B-3 AT  $P_e = 25.7$  kb, AND (C) PRESSED TNT AT  $P_e = 51.8$  kb. [6.53  $\mu\text{sec}$  BETWEEN SUCCESSIVE OUTLINES.]

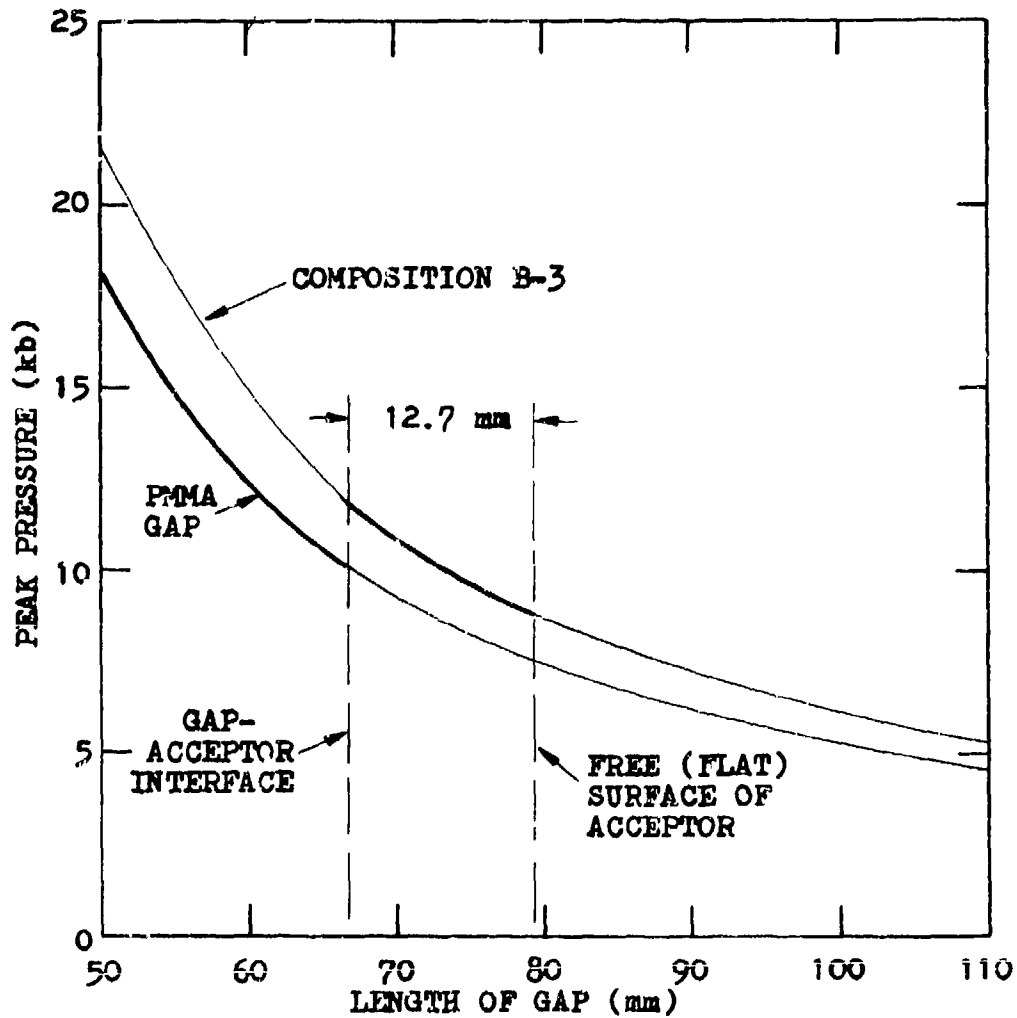


FIG. 14. METHOD OF DETERMINING THE STRESS IN THE ACCEPTOR FROM WHICH THE FREE-SURFACE VELOCITY OF AN UNREACTING ACCEPTOR ( $U^*$ ) CAN BE CALCULATED.

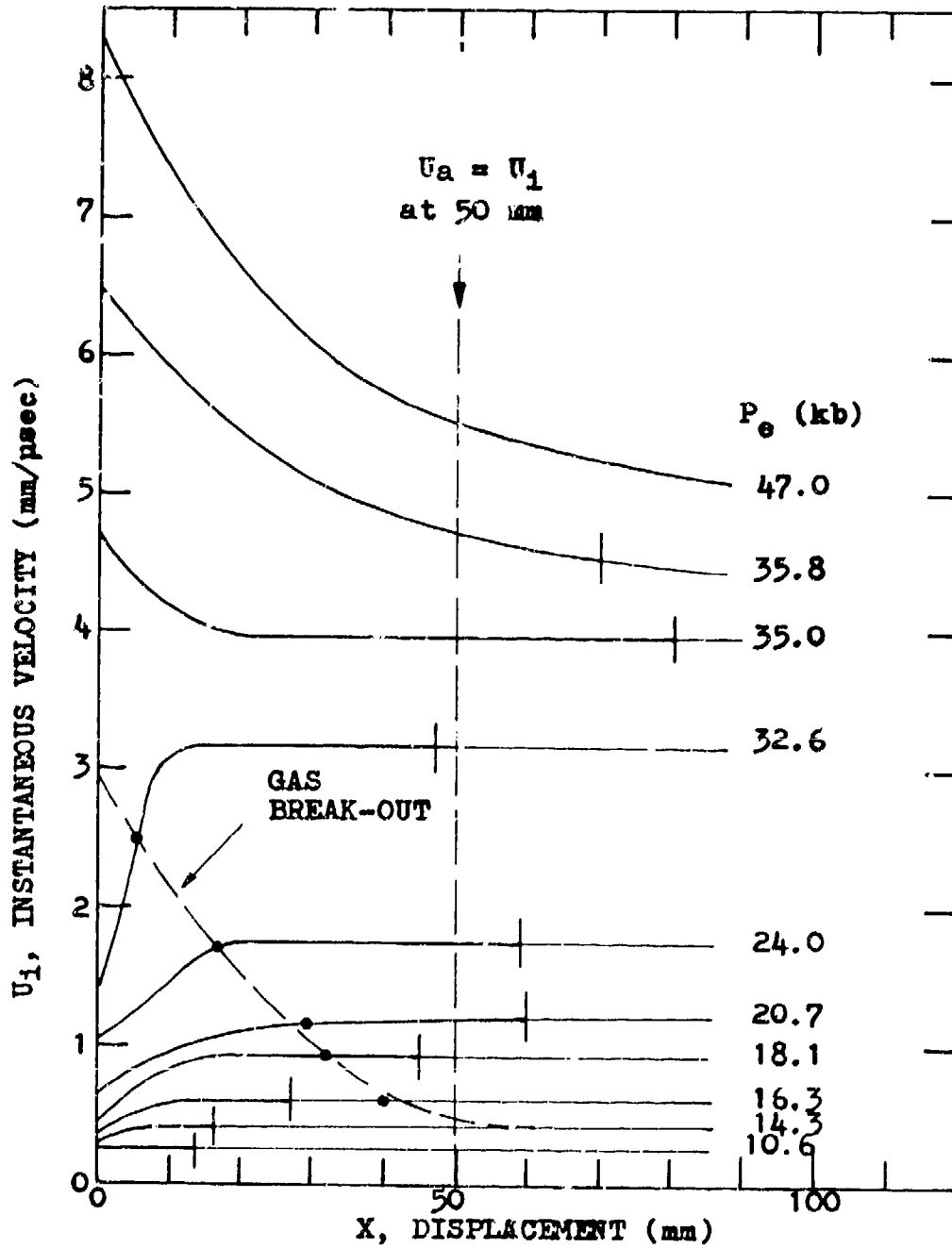


FIG. 15. INSTANTANEOUS VELOCITY ( $U_1$ ) OF THE ACCEPTOR AS A FUNCTION OF DISPLACEMENT ( $X$ ) FOR COMP B-3 CAST

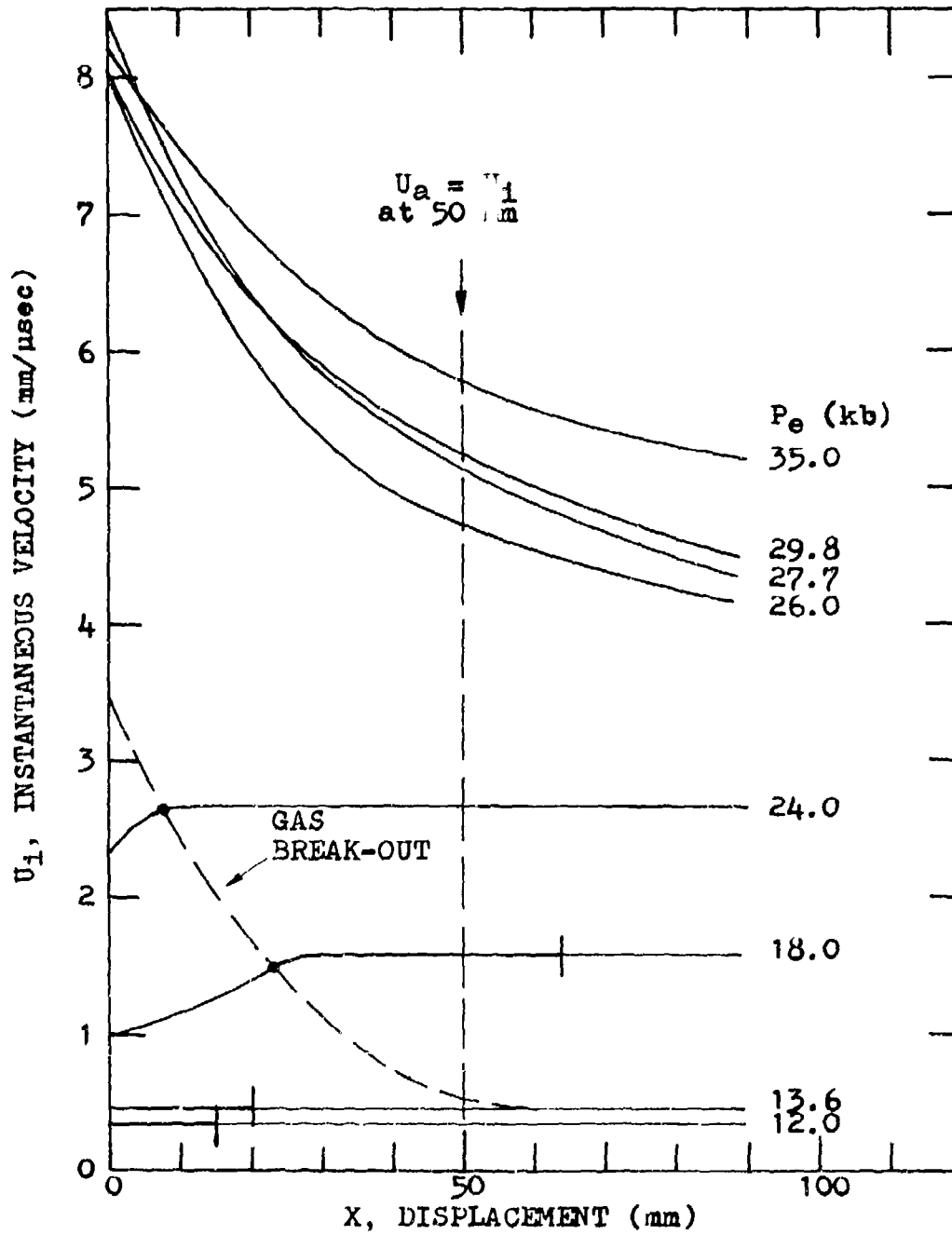


FIG. 16. INSTANTANEOUS VELOCITY ( $U_1$ ) AS A FUNCTION OF DISPLACEMENT ( $X$ ) FOR PRESSED COMP B-3.

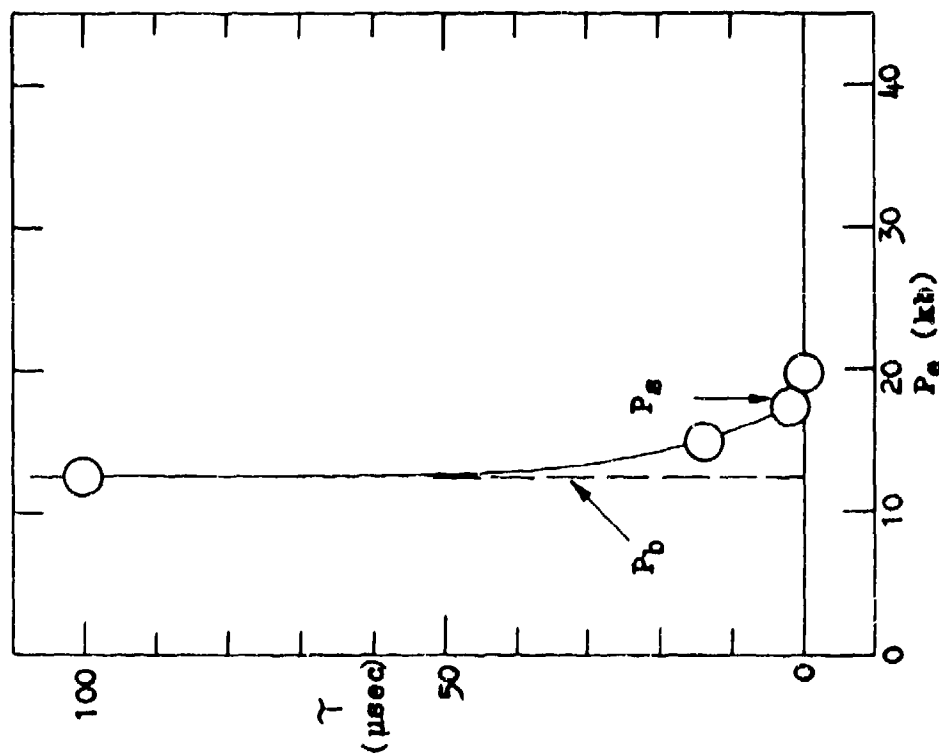
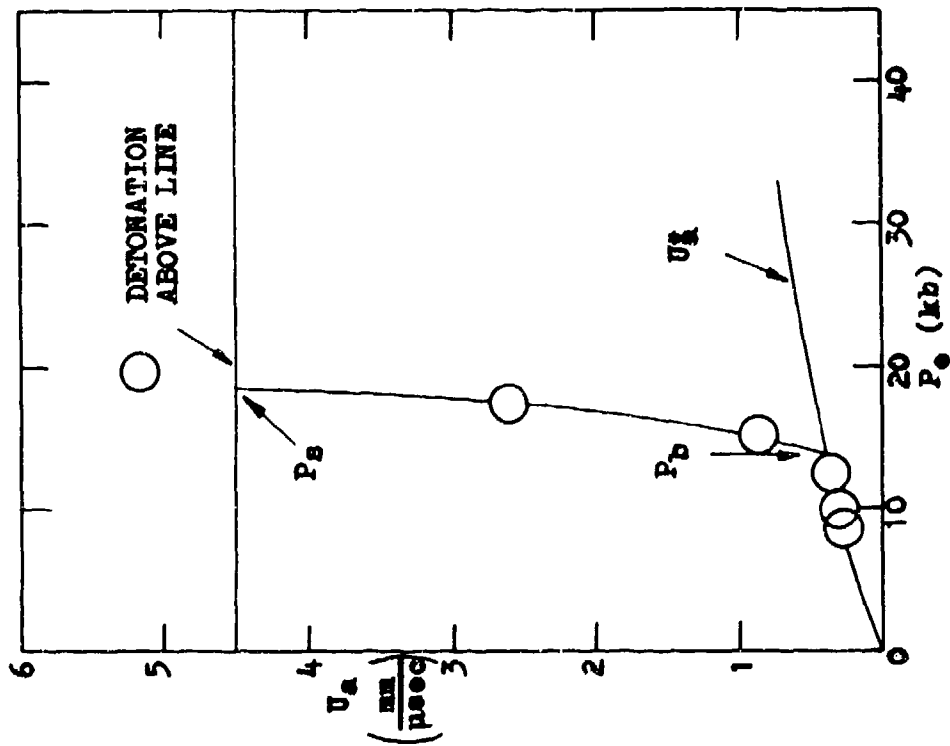


FIG. 17. BREAK-OUT TIME ( $\tau$ ) AND ACCEPTOR VELOCITY ( $U_a$ ) AS FUNCTIONS OF THE ENTERING SHOCK STRESS ( $P_e$ ) FOR TETRYL.

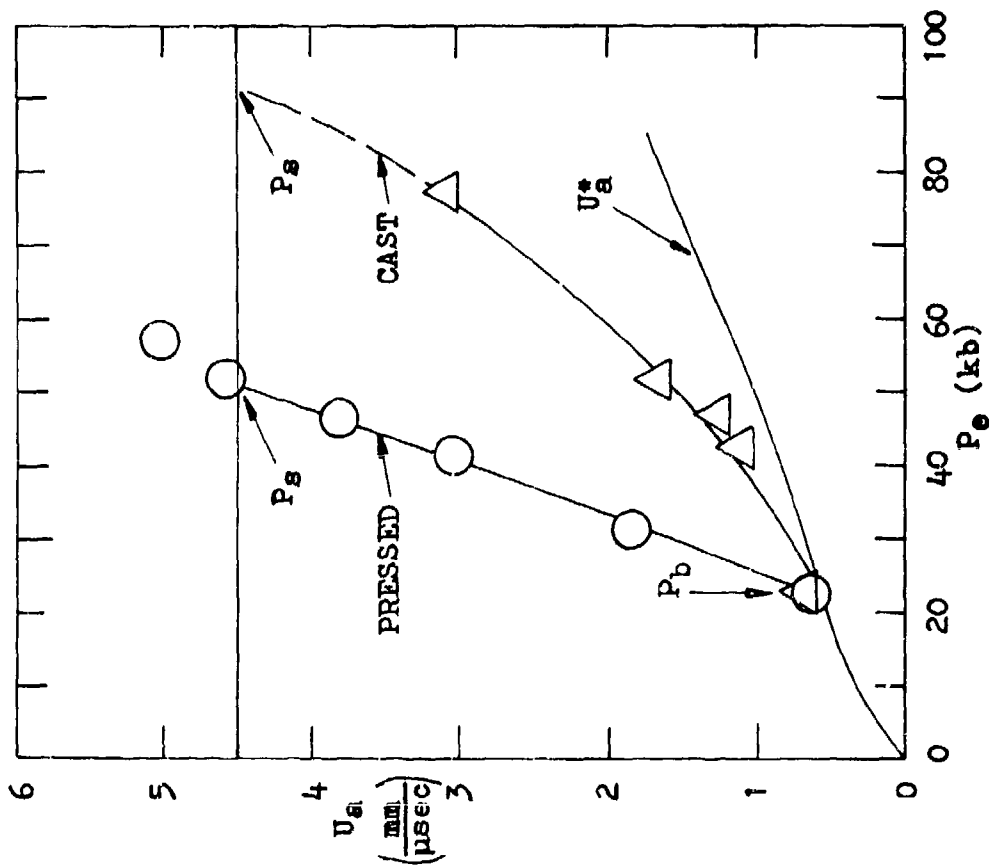


FIG. 18.  $U_a$  AS A FUNCTION OF  $P_e$  FOR PRESSED AND CAST TNT. [THE BREAK-OUT TIME (T) COULD NOT BE DETERMINED FOR THIS EXPLOSIVE.]

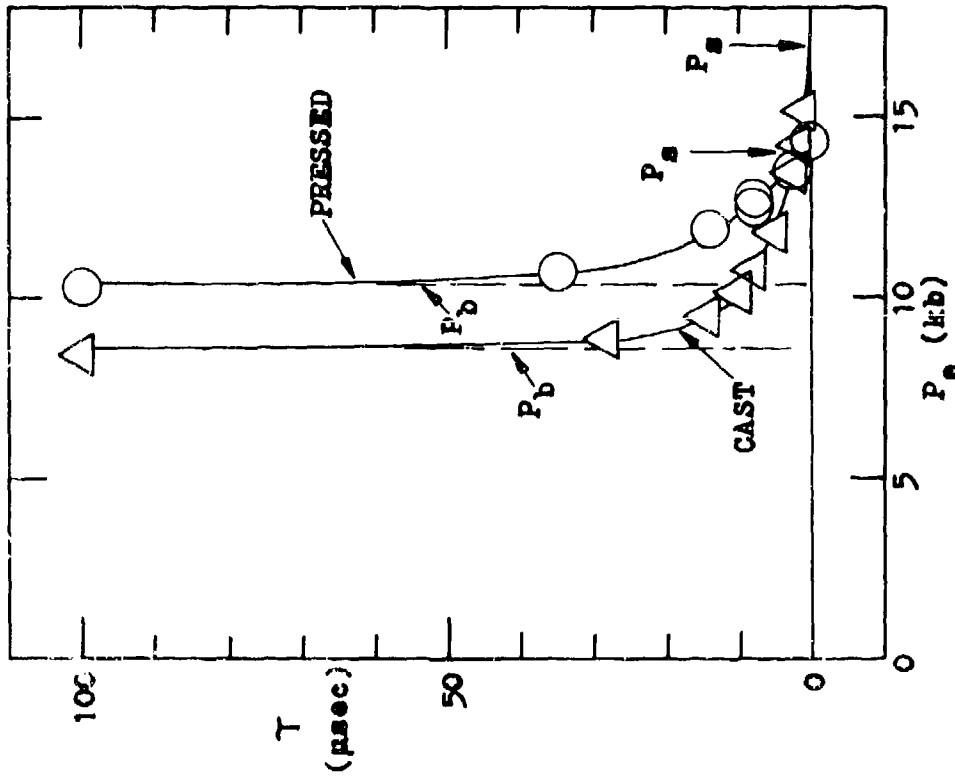
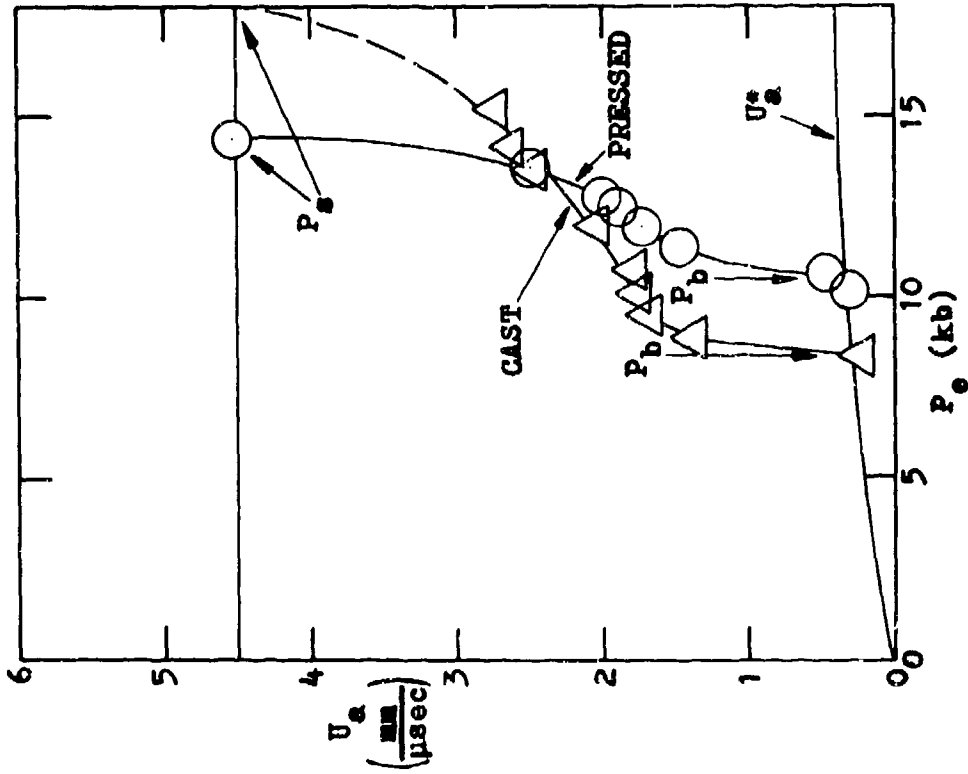


FIG. 19.  $T$  AND  $U_a$  AS FUNCTIONS OF  $P_e$  FOR PRESSED AND CAST PENTOLITE.

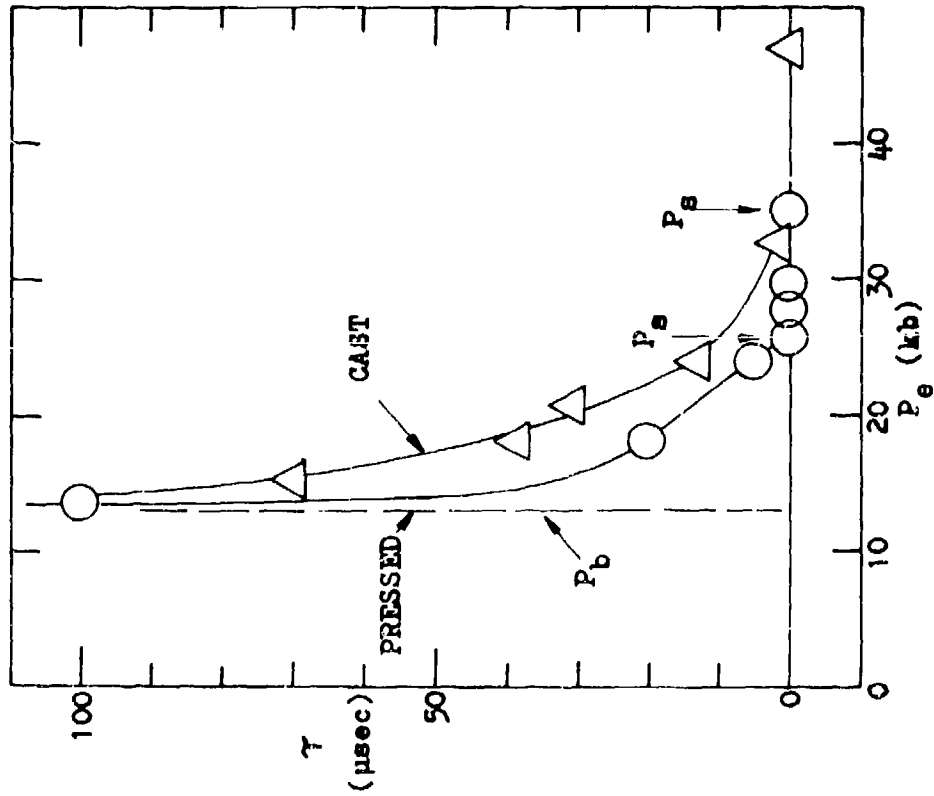
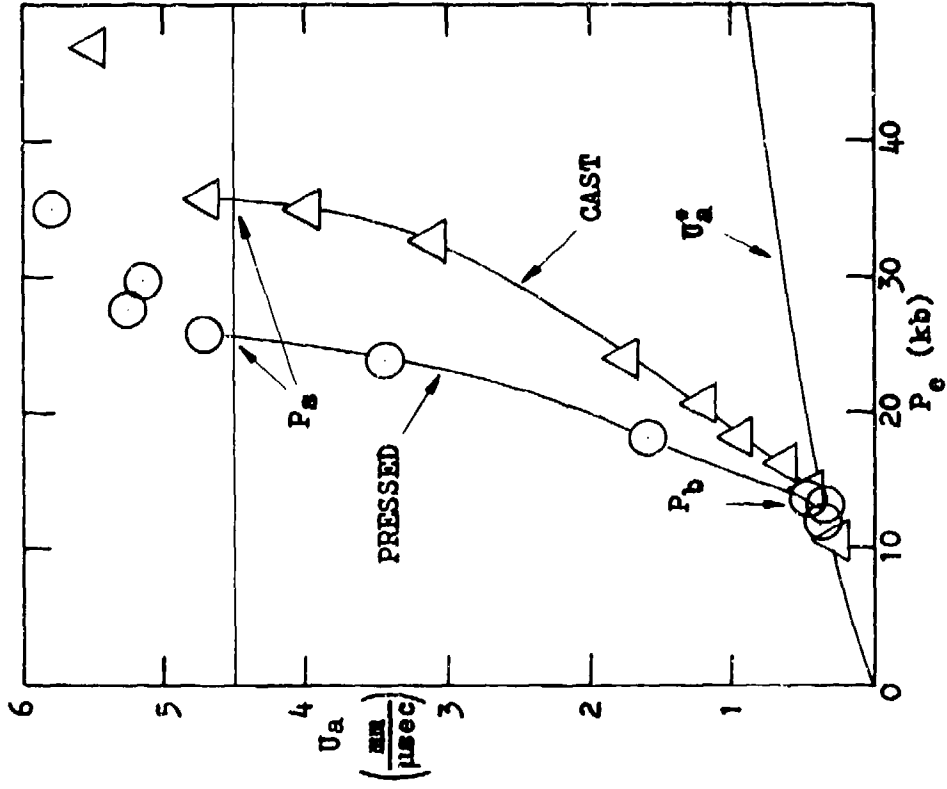


FIG. 20.  $\tau$  AND  $U_a$  AS FUNCTIONS OF  $P_e$  FOR PRESSED AND CAST COMP B-3.

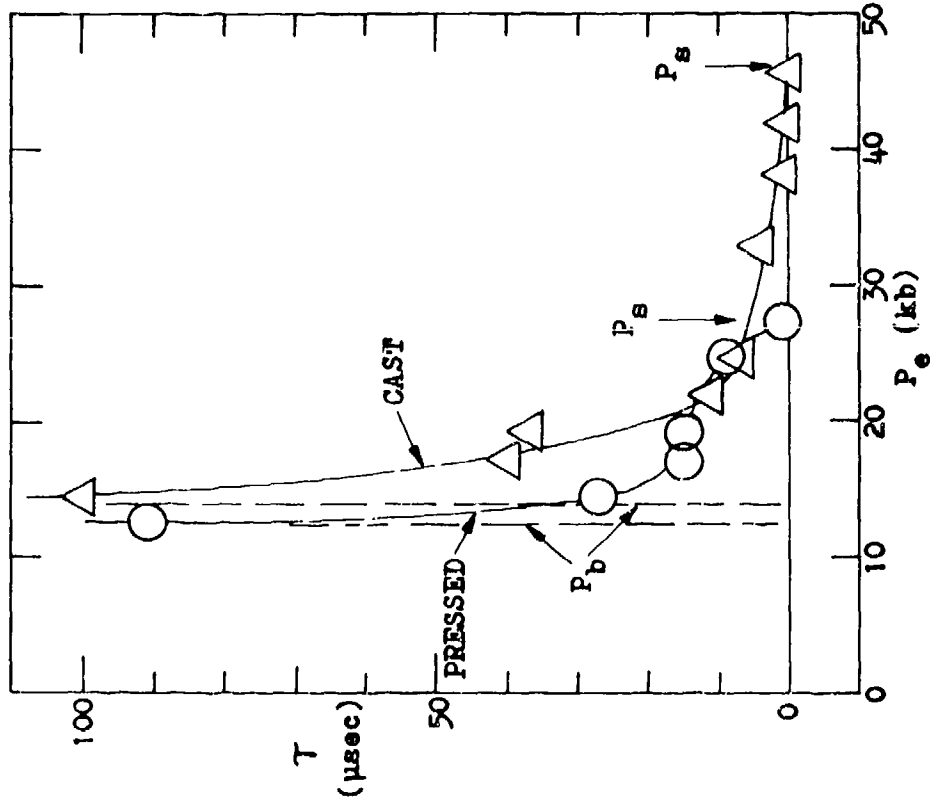
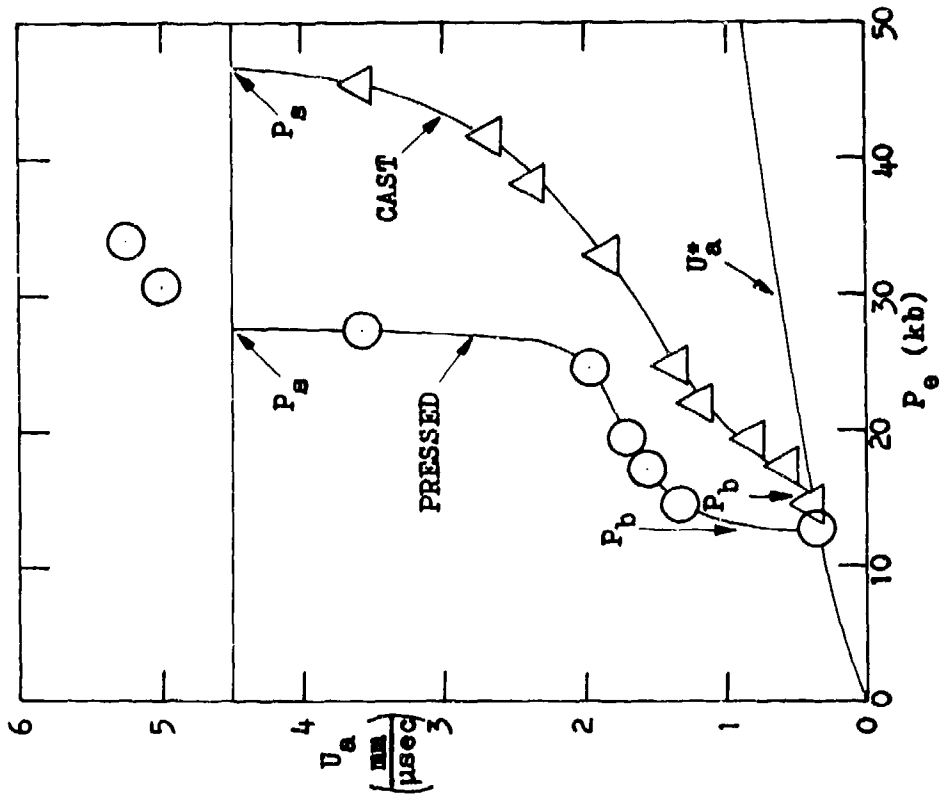


FIG. 21.  $T$  AND  $U_a$  AS FUNCTIONS OF  $P_e$  FOR CAST AND PRESSED 60/40 CYCLOTOL.

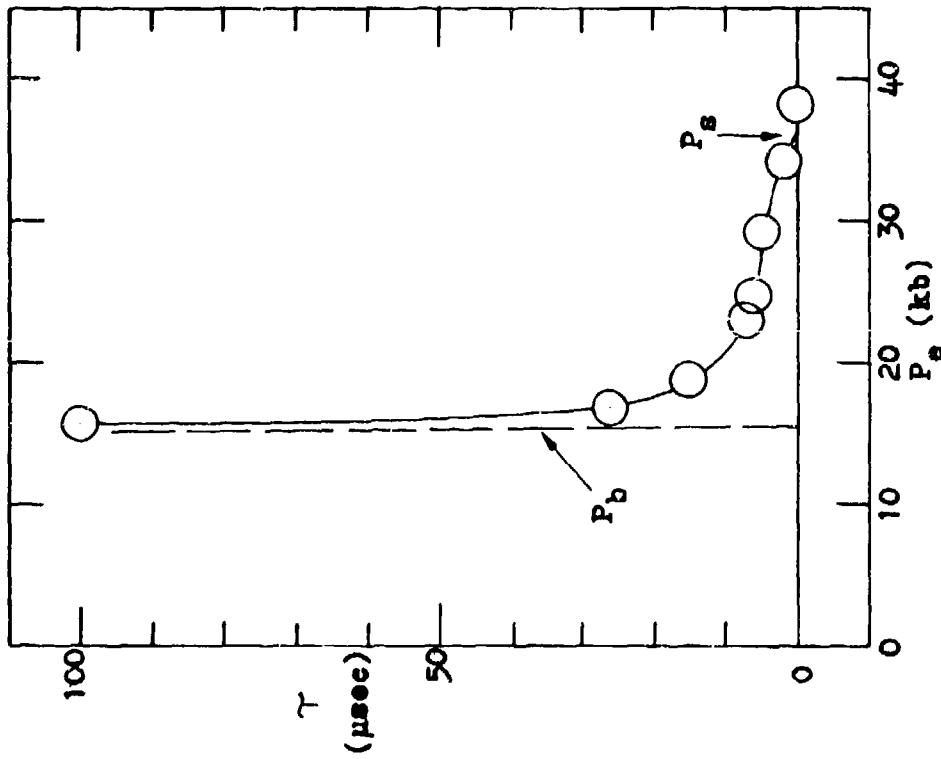
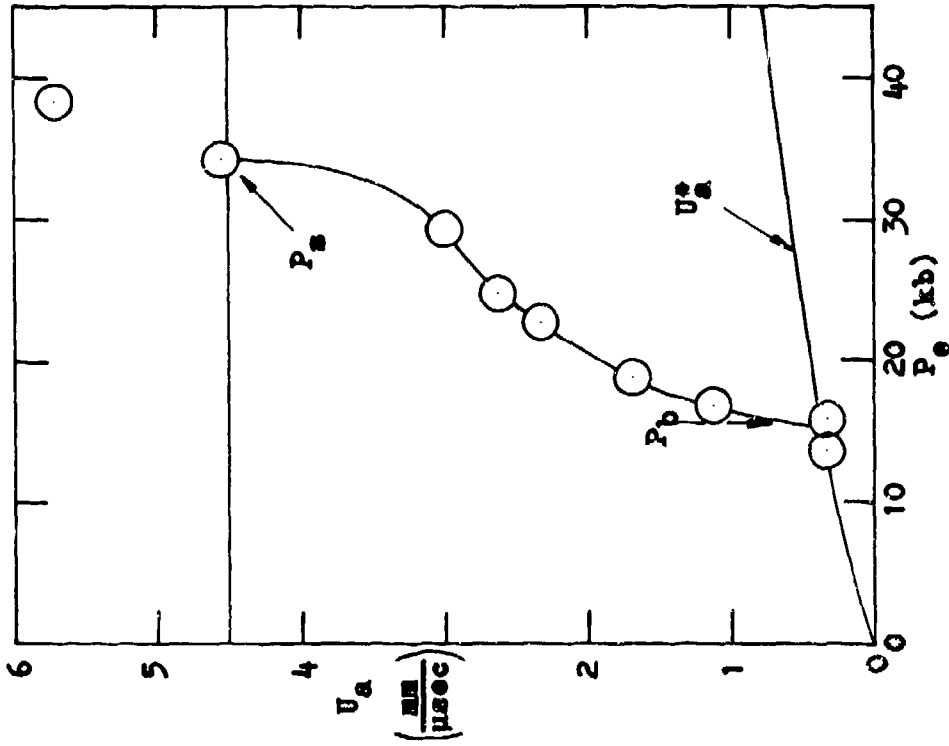


FIG. 22.  $\tau$  AND  $U_a$  AS FUNCTIONS OF  $P_e$  FOR PBX 9404.

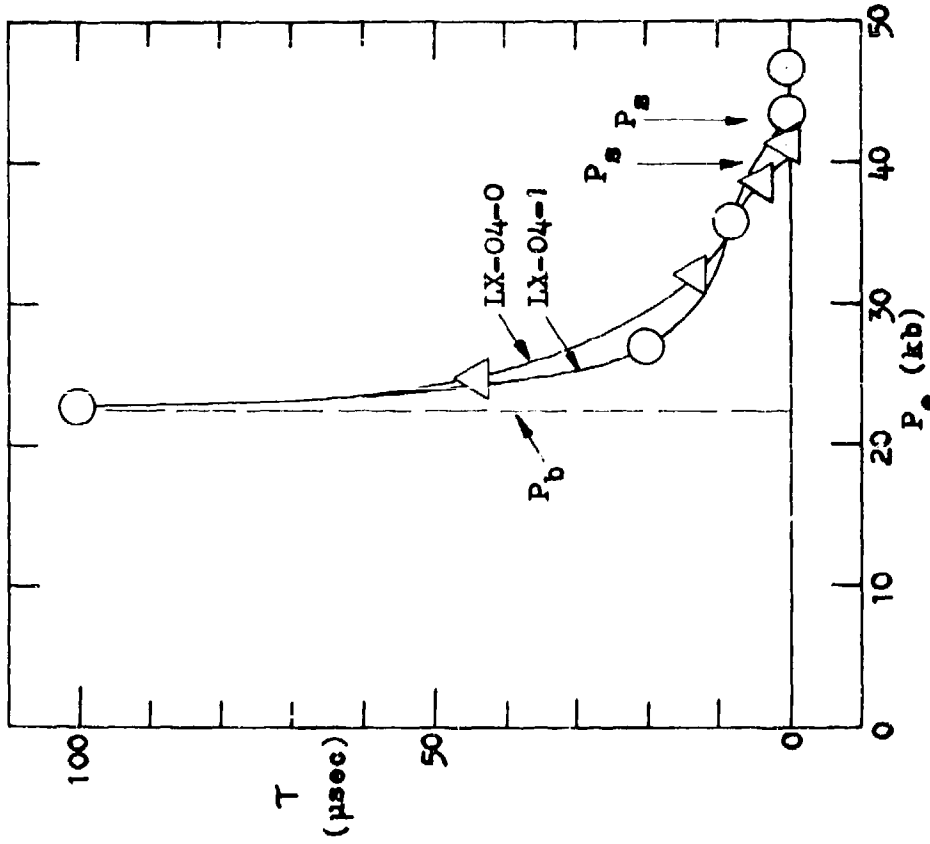
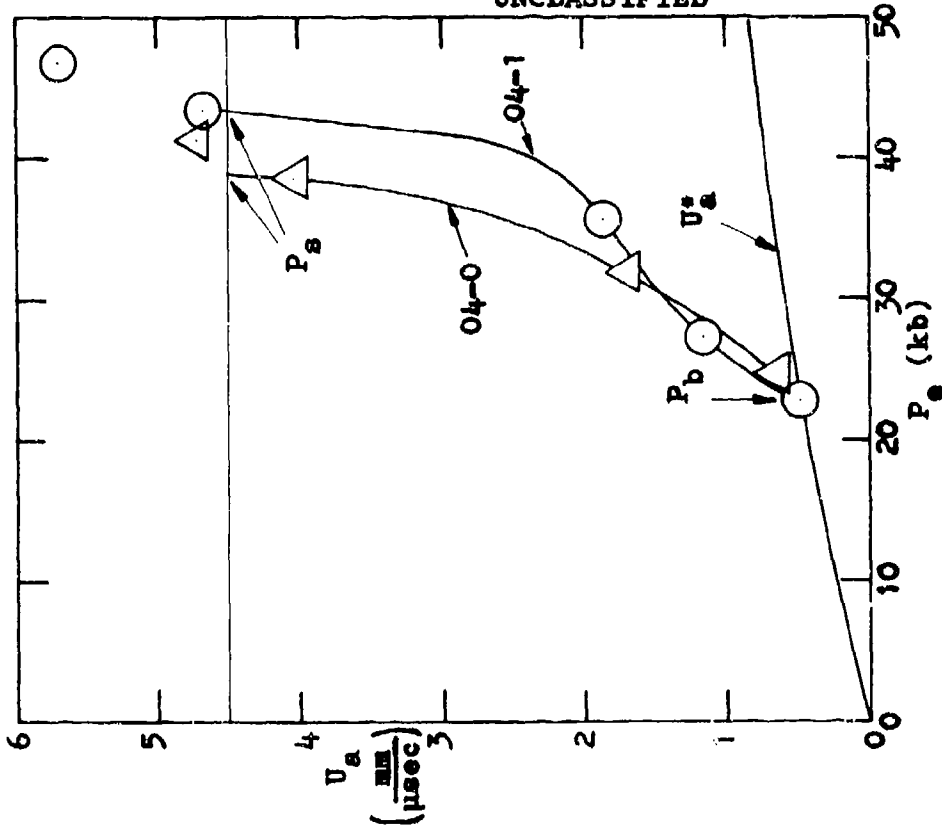


FIG. 23.  $T$  AND  $U_a$  AS FUNCTIONS OF  $P_e$  FOR LX-04-0 AND LX-04-1.

DISTRIBUTION

	Copies
Chief, Bureau of Naval Weapons Department of the Navy Washington , D. C. 20360	
DLI-3	4
RRRE-5	1
RMMO-611	1
RMMO-621	1
RMMO-622	1
RMMO-13	1
RREN-32	1
RRRE-6	1
RRRE-51	1
RMMO-523	1
Director Special Projects Office Department of the Navy Washington , D. C. 20360	
SP-20	1
Superintendent Naval Post Graduate School Monterey, California 93940	
	1
Office of Naval Research Department of the Navy Washington , D. C. 20360	
	2
Commander U. S. Naval Ordnance Test Station China Lake, California 93557	
Code 556	1
Technical Library	1
H. D. Mallory	1
H. Gryting	1
R. Plauson	1
Director Naval Research Laboratory Washington , D. C. 20390	
Technical Information Section	2
Commander U. S. Naval Weapons Laboratory Dahlgren, Virginia 22448	
Technical Library	2
Weapons Laboratory	1
Terminal Ballistics Laboratory	1
D. Abernathy	1
J. Talley	1

NOLTR 64-53  
UNCLASSIFIED

	Copies
U.S. Department of Commerce U.S. Clearinghouse for Scientific & Tech. Info. Sills Building, 5285 Port Royal Road Springfield, Virginia 22151	100
Underwater Explosions Research Division David Taylor Model Basin Portsmouth, Virginia 23709	1
Commanding Officer U. S. Naval Weapons Station Yorktown, Virginia 23491 R & D Division	2
Commanding Officer U. S. Naval Propellant Plant Indian Head, Maryland 20640 Technical Library	1
Commanding Officer U. S. Naval Ordnance Plant Macon, Georgia 31201	1
Commanding Officer Naval Ammunition Depot Crane, Indiana	1
Commanding Officer U. S. Naval Ammunition Depot Navy Number Six Six (66) c/o Fleet Post Office San Francisco, California 96612 Quality Evaluation Laboratory	1
Commanding Officer U. S. Naval Underwater Ordnance Station Newport, Rhode Island 02844	1
Commanding Officer U. S. Naval Weapons Evaluation Facility Kirtland Air Force Base Albuquerque, New Mexico 87117	1
Commanding Officer U. S. Naval Explosive Ordnance Disposal Facility Indian Head, Maryland 20640 Library Division	1

	Copies
Army Material Command Department of the Army Washington , D. C. 20315 R & D Division	1
Commander Army Rocket & Guided Missile Command Redstone Arsenal, Huntsville, Alabama 35809 ORDXR-RH	1
Commanding Officer U. S. Army Missile Command Redstone Arsenal, Alabama 35809	1
Commanding General Picatinny Arsenal Dover, New Jersey 07801	
SMUPA-W	1
SMUPA-G	1
SMUPA-VL	1
SMUPA-VE	1
SMUPA-VC	1
SMUPA-DD	1
SMUPA-DR	2
SMUPA-DR-4	1
SMUPA-DW	1
SMUPA-TX	1
SMUPA-TW	1
SMUPA-V	1
Commanding Officer Harry Diamond Laboratory Connecticut Ave & Van Ness St., N. W. Washington , D. C. 20438 Ordnance Development Lab M. Lipnick (Code 005)	1 1
Army Research Office Box CM Duke Station Durham, North Carolina 27706	1
Army Engineer Research & Development Labs. Ft. Belvoir, Virginia 22060 STINFO Branch Z. Harvalik	2 1

	Copies
Commanding Officer Aberdeen Proving Ground Aberdeen, Maryland 21005 BRL Tech. Libr.	1
R. J. Eichelberger	1
M. Sultanoff	1
G. Hauver	1
Commanding General Redstone Arsenal Huntsville, Alabama 35809 Technical Library	1
Commanding Officer Frankford Arsenal Philadelphia, Pa. 19137 Library	1
Chief of Staff U. S. Air Force Washington, D. C. 20350 AFORD-AR	1
Systems Engineering Group (RTD) Wright-Patterson Air Force Base, Ohio 45433 SEPIR	1 2
Headquarters, Air Proving Ground Center U. S. Air Force, ARDC Eglin Air Force Base, Florida 32542 PGTRI, Technical Library	1
Commander Air Research & Development Command Andrews Air Force Base Washington, D. C. 20331	1
Director, Applied Physics Laboratory Johns Hopkins University 8621 Georgia Avenue Silver Spring, Maryland 20910 F. L. Welanetz E. Nooker F. Hill Library	1 1 1 1
Atomic Energy Commission Washington 25, D. C. DMA	1

NOLTR 64-53  
UNCLASSIFIED

	Copies
Director U. S. Bureau of Mines Explosives Research Center 4800 Forbes Avenue Pittsburgh , Pennsylvania 15213	1
R. W. VanDolah	1
F. C. Gibson	1
C. Mason	1
Defense Documentation Center Cameron Station Alexandria, Virginia 22314 TIPCR	20
National Aeronautics & Space Admin. Goddard Space Flight Center Greenbelt, Maryland 20771	1
Lawrence Radiation Laboratory P. O. Box 808 Livermore, California 94551 Technical Information Division	1
M. L. Wilkins	1
G. D. Dorough	1
R. Duff	1
E. James, Jr.	1
J. Kury	1
Mr. Wassly	1
Director, Los Alamos Scientific Lab. P. O. Box 1663 Los Alamos, New Mexico 87544 Library	1
A. W. Campbell	1
W. C. Davis	1
L. C. Smith	1
J. B. Ramsay	1
J. R. Travis	1
C. L. Mader	1
D. P. MacDougall	1
Berlyn Brixner	1
Sandia Corporation P. O. Box 969 Livermore, California	1
Sandia Corporation P. O. Box 5400 Albuquerque, New Mexico 87115 Taylor Abegg	1
W. B. Benedick	1

NOLTR 64-53  
UNCLASSIFIED

	Copies
Alleghaney Ballistics Laboratory Cumberland, Maryland 21501	1
Flare-Northern Division Atlantic Research Corporation 19701 W. Goodvale Road Saugus, California	1
Atlas Chemical Industries, Inc. Tamaqua, Pennsylvania 18252 Mr. B. Gay, Valley Forge, Pa.	1 1
Atlantic Research Corporation Flare-Northern Division P. O. Box 175 West Hanover, Massachusetts Mr. J. A. Smith, Sec. Off.	1
Hercules Powder Company Port Ewen, New York 12466	1
Martin Company Armament Section Orlando, Florida 32800	1
Thiokol Chemical Corp. Redstone Division Redstone, Alabama 35809	1
Shock Hydrodynamics, Inc. 15010 Ventura Boulevard Sherman Oaks, California 91403 L. Zernow	1 1
Stanford Research Institute Menlo Park, California 94025 Poulter Lab. Library A. B. Amster M. W. Evans M. Cowperthwaite J. Erkman Z. Pressman	1 1 1 1 1 1
Thiokol Chemical Corp. Hunter Bristol Division Bristol, Pennsylvania	1
McCormick-Selph Associates Hollister Airport Hollister, California	1

	Copies
Lockheed Missiles and Space Division Joegels Road Sunnyvale, California	1
R. Stresau Laboratory Spooner, Wisconsin 54801	1
John Jay Hopkins Laboratory General Atomic San Diego, California B. B. Dunne	1
Department of Physics Washington State University Pullman, Washington 99163 G. E. Duvall	1
Commanding Officer U. S. Naval Ordnance Laboratory Corona, California 91720 R: Hillver R: Higuera Commanding Officer U. S. Naval Ammunition Depot Concord, California 94520 Quality Evaluation Laboratory	1 1 1 1
Commander Army Rocket and Guided Missile Agency Redstone Arsenal, Huntsville, Alabama 35809 ORDXR-RH	1
U.S. Naval Academy Annapolis, Md. Cdr. Geiger	1
Philco Ford Road Newport Beach, Calif. 92600 M. Boyer	1 1
Honeywell, Inc. 600 Second Street North Hopkins, Minnesota 55343	1
Bermite Powder Co. Saugus, California 91350	1
E. I. duPont deNemours & Co. Explosives Dept. Gibbstown, New Jersey 08027 L. Courson	1

	Copies
Aerojet-General Corp. 11711 Woodruff Avenue Downey, California 90241 H. J. Fisher, Ordnance Div.	1
Atlantic Research Corp. Shirley Highway & Edsall Road Alexandria, Virginia A. Macek	1
Rohm & Haas Co. Redstone Arsenal Research Div. Huntsville, Alabama 35808 K. Ockert H. Shuey	1 1
IIT Research Institute 10 West 35th Street Chicago, Illinois 60616 H. Napadensky J. Kennedy	1 1
University of Utah Inst. of Metals and Explosives Research Salt Lake City, Utah M. A. Cook	1
Intermountain Research & Engineering Co., Inc. 1635 Pioneer Road Salt Lake City 4, Utah Dr. Pack	1
Explosiform, Inc. 1001 Skyline Blvd San Francisco, California 94132 J. Savitt	1
Combustion & Explosives Research, Inc. Oliver Building Pittsburgh, Pennsylvania W. Gordon	1

**UNCLASSIFIED**

Security Classification

DOCUMENT CONTROL DATA - R&D		
<i>(Security classification of title, body of abstract and indexing annotation must be entered when the overall report is classified)</i>		
1 ORIGINATING ACTIVITY <i>(Corporate author)</i> <b>Naval Ordnance Laboratory White Oak, Md.</b>		2a. REPORT SECURITY CLASSIFICATION <b>Unclassified</b>
		2b. GROUP ---
3 REPORT TITLE <b>Initiation of Reaction in Explosives by Shocks</b>		
4. DESCRIPTIVE NOTES <i>(Type of report and inclusive dates)</i>		
5 AUTHOR(S) <i>(Last name, first name, initial)</i> <b>Liddiard, T. P. Jacobs, S. J.</b>		
6 REPORT DATE <b>4 October 1965</b>	7a. TOTAL NO OF PAGES <b>44</b>	7b. NO OF REFS <b>14</b>
8a. CONTRACT OR GRANT NO.	9a. ORIGINATOR'S REPORT NUMBER(S) <b>NOLTR 64-53</b>	
b. PROJECT NO. <b>NOL Task 260 BuWeps Task Assignment RMMO 51 d042/212-1/F009-08-02</b>	9b. OTHER REPORT NO(S) <i>(Any other numbers that may be assigned this report)</i> ---	
10. AVAILABILITY/LIMITATION NOTICES <b>Qualified requestors may obtain from DDC.</b>		
11. SUPPLEMENTARY NOTES	12. SPONSORING MILITARY ACTIVITY <b>Bureau of Naval Weapons</b>	
13. ABSTRACT <b>Several solid high explosives are subjected to shocks of moderate amplitude, 10-50 kb. In general, these shocks are strong enough to cause chemical reaction, but not full detonation. The shock-producing system used is essentially that of the NOL standardized gap test. The acceptors (50.8 mm diam x 12.7 mm thick) are much shorter and are unconfined. Examples (photographic sequences) are shown of the acceptor response of several explosives at various entering shock pressures (stresses). The stress in the acceptor which just produces detectable reaction is determined from a plot of the break-out time of gaseous products of reaction from the acceptor as a function of the entering stress. The stress at which detonation is just produced in the acceptors is also determined. Threshold values for burning and for detonation also are obtained from graphs of the velocity of the acceptor undergoing chemical reaction as a function of the entering stress. Near the threshold for burning the velocity of the acceptor surface is very sensitive to the amount of reaction. This results in an abrupt change of slope in the velocity-stress curve at the critical stress for burning. The thresholds for burning and for detonation are compared with the 50% firing stresses obtained with the standardized gap test.</b>		

DD FORM 1473

**UNCLASSIFIED**  
Security Classification

14. KEY WORDS	LINK A		LINK B		LINK C	
	ROLE	WT	ROLE	WT	ROLE	WT
<b>Initiation</b> <b>Shock Wave</b> <b>Gap Test</b> <b>Detonation</b>						

**INSTRUCTIONS**

1. **ORIGINATING ACTIVITY:** Enter the name and address of the contractor, subcontractor, grantee, Department of Defense activity or other organization (*corporate author*) issuing the report.
- 2a. **REPORT SECURITY CLASSIFICATION:** Enter the overall security classification of the report. Indicate whether "Restricted Data" is included. Marking is to be in accordance with appropriate security regulations.
- 2b. **GROUP:** Automatic downgrading is specified in DoD Directive 5200.10 and Armed Forces Industrial Manual. Enter the group number. Also, when applicable, show that optional markings have been used for Group 3 and Group 4 as authorized.
3. **REPORT TITLE:** Enter the complete report title in all capital letters. Titles in all cases should be unclassified. If a meaningful title cannot be selected without classification, show title classification in all capitals in parenthesis immediately following the title.
4. **DESCRIPTIVE NOTES:** If appropriate, enter the type of report, e.g., interim, progress, summary, annual, or final. Give the inclusive dates when a specific reporting period is covered.
5. **AUTHOR(S):** Enter the name(s) of author(s) as shown on or in the report. Enter last name, first name, middle initial. If military, show rank and branch of service. The name of the principal author is an absolute minimum requirement.
6. **REPORT DATE:** Enter the date of the report as day, month, year, or month, year. If more than one date appears on the report, use date of publication.
- 7a. **TOTAL NUMBER OF PAGES:** The total page count should follow normal pagination procedures, i.e., enter the number of pages containing information.
- 7b. **NUMBER OF REFERENCES:** Enter the total number of references cited in the report.
- 8a. **CONTRACT OR GRANT NUMBER:** If appropriate, enter the applicable number of the contract or grant under which the report was written.
- 8b, 8c, 8d. **PROJECT NUMBER:** Enter the appropriate military department identification, such as project number, subproject number, system numbers, task number, etc.
- 9a. **ORIGINATOR'S REPORT NUMBER(S):** Enter the official report number by which the document will be identified and controlled by the originating activity. This number must be unique to this report.
- 9b. **OTHER REPORT NUMBERS:** If the report has been assigned any other report numbers (*either by the originator or by the sponsor*), also enter this number(s).
10. **AVAILABILITY/LIMITATION NOTICES:** Enter any limitation on further dissemination of the report, other than those

imposed by security classification, using standard statements such as:

- (1) "Qualified requesters may obtain copies of this report from DDC."
- (2) "Foreign announcement and dissemination of this report by DDC is not authorized."
- (3) "U. S. Government agencies may obtain copies of this report directly from DDC. Other qualified DDC users shall request through \_\_\_\_\_."
- (4) "U. S. military agencies may obtain copies of this report directly from DDC. Other qualified users shall request through \_\_\_\_\_."
- (5) "All distribution of this report is controlled. Qualified DDC users shall request through \_\_\_\_\_."

If the report has been furnished to the Office of Technical Services, Department of Commerce, for sale to the public, indicate this fact and enter the price, if known.

11. **SUPPLEMENTARY NOTES:** Use for additional explanatory notes.

12. **SPONSORING MILITARY ACTIVITY:** Enter the name of the departmental project office or laboratory sponsoring (*paying for*) the research and development. Include address.

13. **ABSTRACT:** Enter an abstract giving a brief and factual summary of the document indicative of the report, even though it may also appear elsewhere in the body of the technical report. If additional space is required, a continuation sheet shall be attached.

It is highly desirable that the abstract of classified reports be unclassified. Each paragraph of the abstract shall end with an indication of the military security classification of the information in the paragraph, represented as (TS), (S), (C), or (U).

There is no limitation on the length of the abstract. However, the suggested length is from 150 to 225 words.

14. **KEY WORDS:** Key words are technically meaningful terms or short phrases that characterize a report and may be used as index entries for cataloging the report. Key words must be selected so that no security classification is required. Identifiers, such as equipment model designation, trade name, military project code name, geographic location, may be used as key words but will be followed by an indication of technical context. The assignment of links, roles, and weights is optional.

Naval Ordnance Laboratory, White Oak, Md.  
(NOL technical report 64-53)  
INITIATION OF REACTION IN EXPLOSIVES BY  
SHOCKS, by T. P. Liddiard, jr. and S. J.  
Jacobs. 4 Oct. 1965. 44p. illus., charts.  
tables. NOL task 260. BuWeps task RMAO 51-  
042/212-1/F009-08-02.

UNCLASSIFIED

Several solid high explosives are subjected to shocks of 10-50 kb. Examples of photographic sequences are shown of the acceptor response at various entering shock stresses. Techniques are described by which the stress just causing detectable burning is obtained. The stress at which detonation is just produced also is determined. The results are compared with the 50% firing stresses obtained with the standardized gap test.

1. Explosives - Shock
2. Explosives - Gap tests
- I. Title
- II. Liddiard, Thomas P., jr.
- III. Jacobs, Sigmund J., jr. author
- IV. Project
- V. Project

Abstract card is unclassified.

Naval Ordnance Laboratory, White Oak, Md.  
(NOL technical report 64-53)  
INITIATION OF REACTION IN EXPLOSIVES BY  
SHOCKS, by T. P. Liddiard, jr. and S. J.  
Jacobs. 4 Oct. 1965. 44p. illus., charts.  
tables. NOL task 260. BuWeps task RMAO 51-  
042/212-1/F009-08-02.

UNCLASSIFIED

Several solid high explosives are subjected to shocks of 10-50 kb. Examples of photographic sequences are shown of the acceptor response at various entering shock stresses. Techniques are described by which the stress just causing detectable burning is obtained. The stress at which detonation is just produced also is determined. The results are compared with the 50% firing stresses obtained with the standardized gap test.

1. Explosives - Shock
2. Explosives - Gap tests
- I. Title
- II. Liddiard, Thomas P., jr.
- III. Jacobs, Sigmund J., jr. author
- IV. Project
- V. Project

Abstract card is unclassified.

Naval Ordnance Laboratory, White Oak, Md.  
(NOL technical report 64-53)  
INITIATION OF REACTION IN EXPLOSIVES BY  
SHOCKS, by T. P. Liddiard, jr. and S. J.  
Jacobs. 4 Oct. 1965. 44p. illus., charts.  
tables. NOL task 260. BuWeps task RMAO 51-  
042/212-1/F009-08-02.

UNCLASSIFIED

Several solid high explosives are subjected to shocks of 10-50 kb. Examples of photographic sequences are shown of the acceptor response at various entering shock stresses. Techniques are described by which the stress just causing detectable burning is obtained. The stress at which detonation is just produced also is determined. The results are compared with the 50% firing stresses obtained with the standardized gap test.

1. Explosives - Shock
2. Explosives - Gap tests
- I. Title
- II. Liddiard, Thomas P., jr.
- III. Jacobs, Sigmund J., jr. author
- IV. Project
- V. Project

Abstract card is unclassified.

Naval Ordnance Laboratory, White Oak, Md.  
(NOL technical report 64-53)  
INITIATION OF REACTION IN EXPLOSIVES BY  
SHOCKS, by T. P. Liddiard, jr. and S. J.  
Jacobs. 4 Oct. 1965. 44p. illus., charts.  
tables. NOL task 260. BuWeps task RMAO 51-  
042/212-1/F009-08-02.

UNCLASSIFIED

Several solid high explosives are subjected to shocks of 10-50 kb. Examples of photographic sequences are shown of the acceptor response at various entering shock stresses. Techniques are described by which the stress just causing detectable burning is obtained. The stress at which detonation is just produced also is determined. The results are compared with the 50% firing stresses obtained with the standardized gap test.

1. Explosives - Shock
2. Explosives - Gap tests
- I. Title
- II. Liddiard, Thomas P., jr.
- III. Jacobs, Sigmund J., jr. author
- IV. Project
- V. Project

Abstract card is unclassified.